CEDAR Tutorial

Thursday June 28, 2007

State of the art in mesosphere science

John Meriwether
Department of Physics and Astronomy
Clemson University

- 20 years of progress since "ignorasphere" was coined to describe our understanding of the mesosphere region.
- Too many slides! (solution: leave major portion for download version)
- Note the passing of a giant in the field of mesospheric dynamics: Jim Holton, gentleman and scholar.

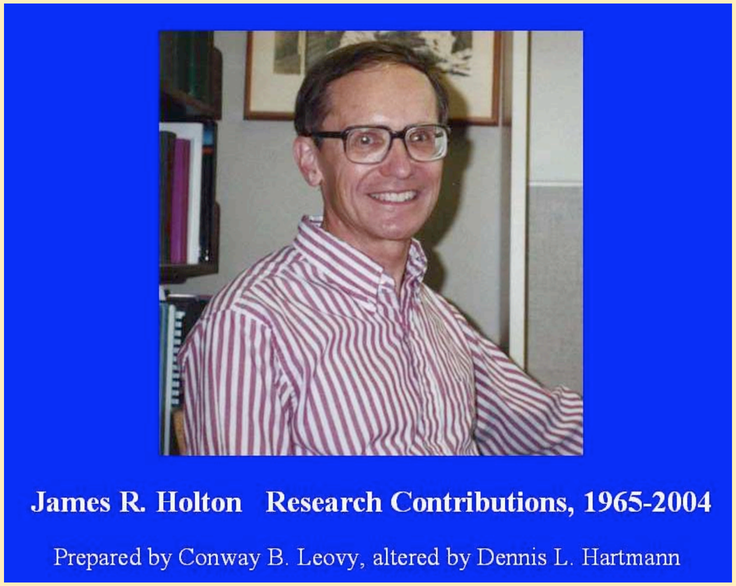

Why observe the Earth and its atmosphere?

- to understand the chemical and physical processes occurring on the land surface, in polar regions, in the oceans, and in the atmosphere.

- to monitor temporal and spatial changes due to natural and anthropogenic causes
(for example, El Nino, ozone hole, greenhouse effect, planetary waves, orographic waves, tidal waves, gravity waves)

- to enable forecasting by getting real-time data

Airglow and lidar observatories at different sites around the globe are studying the aeronomy of the upper atmosphere.

Interesting science and important applications.

Mesosphere major focus for large fraction of these.

What is so interesting about the mesosphere?

- Narrow slice of atmosphere - 20-30 km thickness with marginal dynamical stability
- Marks end of fully mixed atmosphere called “homosphere”
- Highly dynamic region (where waves break and turbulence structures are created)
- Complex region featuring transition from hydrodynamic flow to molecular diffusion
- Observation very contrary to physical intuition:
  - lowest temperatures on Earth in summer polar; warm in winter polar night where there is no solar irradiation - where does this energy come from?

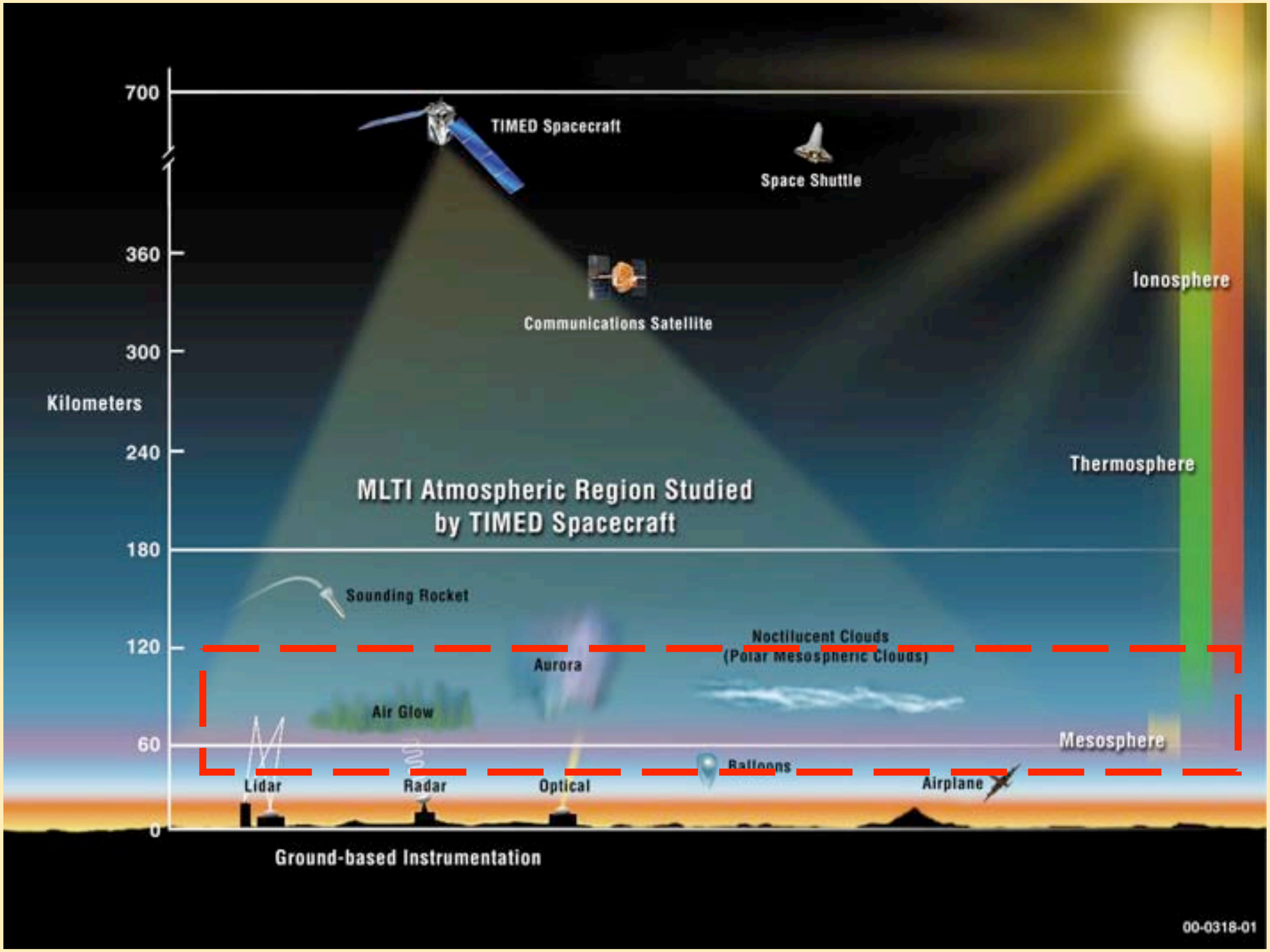

Mesosphere Lower Thermosphere very difficult to reach for ground-based observations - remote sounding most often used

Remote sounding and in situ determination of mesosphere physical properties are performed from many platforms

- Ground
- Balloon payload
- Aircraft
- Rockets
- Space vehicle (shuttle)
- Satellite
- Interplanetary spacecraft

Observing Techniques

- In-situ
  - Balloon-borne radiosondes
  - Rockets
- Ground-based
  - Radar
  - Lidar
  - Passive optics (imager, FPI, spectrograph)
- Satellite

- List not exhaustive
- Concentrate on the basics
- Emphasise the relative strengths and weaknesses
- Observational selection

Rocket Techniques

- Important early source of information on tropical middle atmosphere from Meteorological Rocket Network (MRN)
- **Dropsondes** are instrumented package similar to radiosonde that are carried to 60-80 km by small rocket and released
    - Fall is stabilised and slowed with aid of parachute
    - Temperature and pressure information telemetered to ground
    - Radar tracking gives winds
- **Falling Spheres** are spheres inflated to ~1m diameter and released at heights > 100 km.
- Accelerations tracked by high-precision radars
- Atmospheric density derived from acceleration and known drag coefficients
- Temperatures derived from densities as for Rayleigh lidars
- Winds derived from horizontal accelerations
- Height dependent vertical resolution

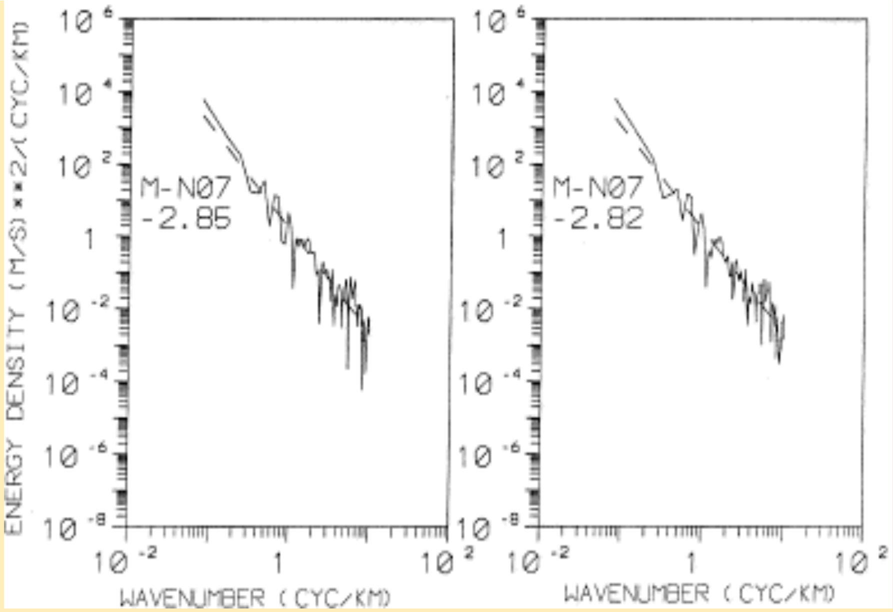

Advantages:

Reliable

Accurate

Limitations:

Expensive

Infrequent

(campaign basis)

Atmospheric Radars

Medium frequency (MF) partial reflection radars

- Frequency ~2-3 MHz
- Winds ~65-100 km (day)
- Winds ~80-100 km (night)

Meteor radars

- Frequency ~30-50 MHz
- Winds ~80 – 105 km
- Temperatures ~90 km

Mesosphere-Stratosphere-Troposphere (MST) radars

- Frequency ~50 MHz (VHF)
- Winds ~2-20 km
- Winds ~60-80 km (day)

Incoherent Scatter radars (ISR)

- Frequency 430 MHz (UHF)
- Arecibo is only IS at tropical latitudes

Slides courtesy, Bob Vincent

TMA chemical release

- Robust: rocket payload releases TMA to produce puffs as tracer of MLT winds using star field and triangulation analysis from two or three ground-stations
- Height profile of winds through MLT region with 1-2 km accuracy
- Launch anytime during night
- High accuracy re wind speed and direction determination
- Comparison with lidar winds shows excellent agreement

Radar Scattering

- Echoes come from vertical gradients in refractive index of air, *n*
- For frequencies > 30 MHz:

$$n = 1 + 0.373\frac{e}{T^2} + 77.6 \cdot 10^{-6}\frac{p}{T} - 40.3\frac{N_e}{f^2}$$

Require fluctuations in

Humidity, *e*

Temperature, *T*

Electron density, *Ne*

Scale of fluctuations or irregularities ~λ/2

~3 m at 50 MHz and ~75 m at 2 MHz

Radar Scattering

- Nature of irregularities is not well known
  - Isotropic turbulence
  - Sharp steps ("Fresnel irregularities")

$$P_r = \frac{\pi P A \alpha \Delta R}{64 R^2} \eta \quad \text{(Volume scatter)}$$

$$P_r = \frac{P A^2 \alpha}{4 \lambda^2 R^2} |\rho|^2 \quad \text{(Fresnel reflection)}$$

- Strength of scatter depends on strength of turbulence, η or on Fresnel reflection coefficient, ρ
- PA is a "figure of merit" for a radar
- P is average transmitted power
- A is antenna area

MST Radars

Equatorial Atmospheric Radar (EAR)
Sumatra, Indonesia (0º)

Versatile and powerful systems for studying atmospheric dynamics with excellent time and height resolution

MU radar, Kyoto, Japan (35ºN)

Jicamarca Observatory, Peru (12ºS)

Performance of MST Radars

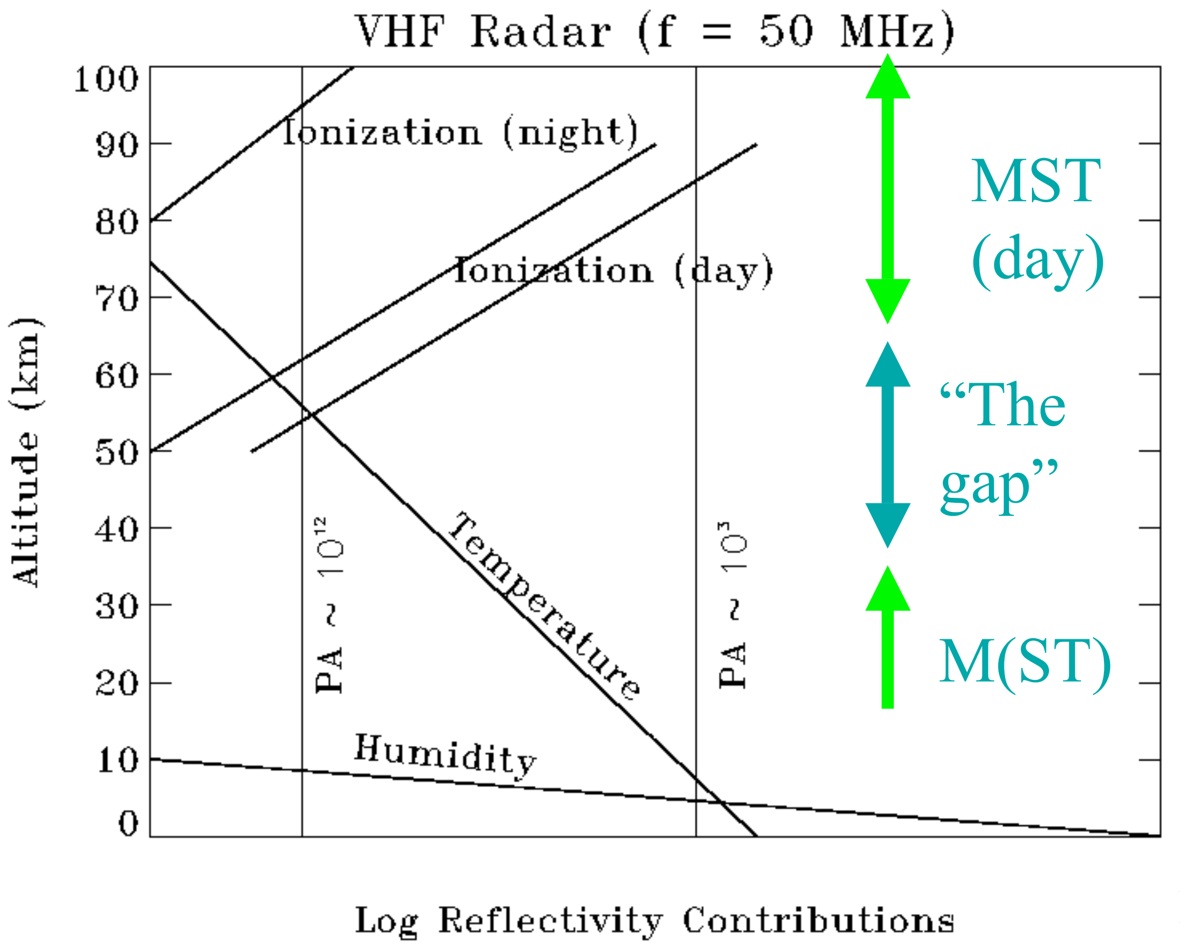

- For good height coverage need:
  - ✓ Large *PA* product
  - ✓ Strong turbulence
- Mesospheric scattering intermittent in time and space

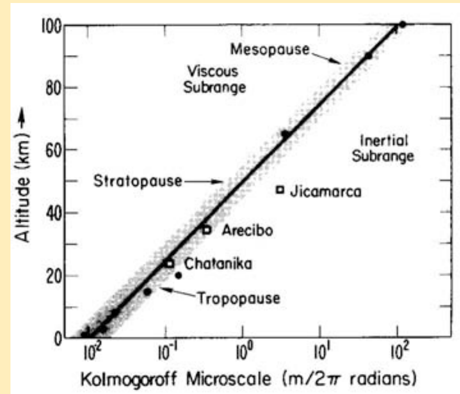

Intense turbulence required to generate mesospheric irregularities

MF Radars

- Strengths
  - Moderate to good range and time resolution
    - range ~ 2 - 4 km
    - time ~ 2 - 5 min
  - Good height coverage
    - 60 - 100 km (day)
    - 80 - 100 km (night)
  - Low power, inexpensive to set up and run
  - Reliable continuous operation
- Use spaced-antenna technique to determine wind velocity
  - Measure motion of diffraction pattern across ground by sampling at 3 spaced antennas
- Measurement of turbulence motions

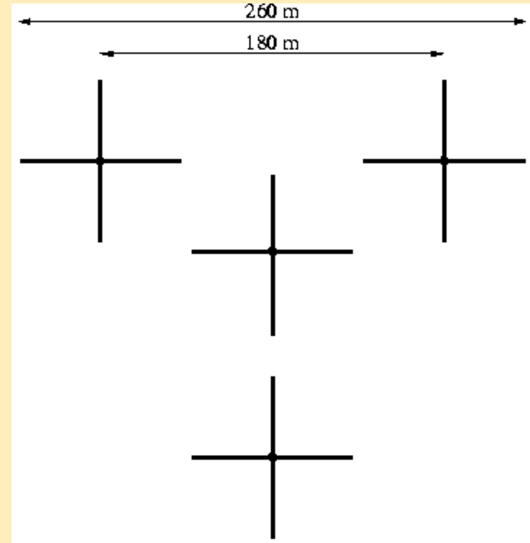

Typical antenna layout

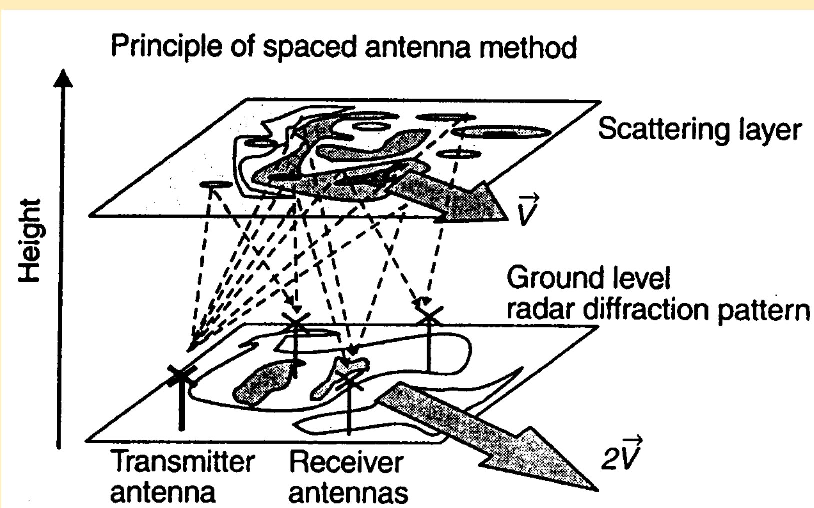

(After Hocking, 1997)

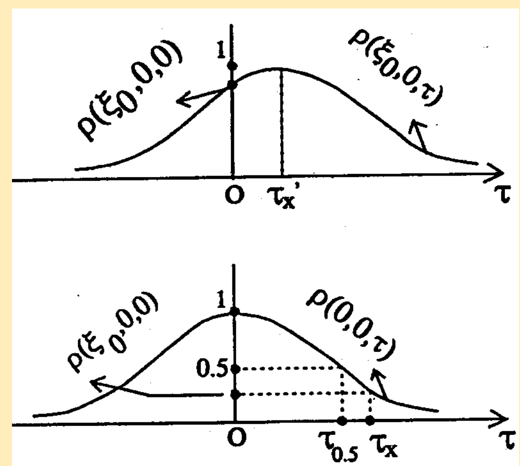

Correlation analysis (After Briggs, 1984)

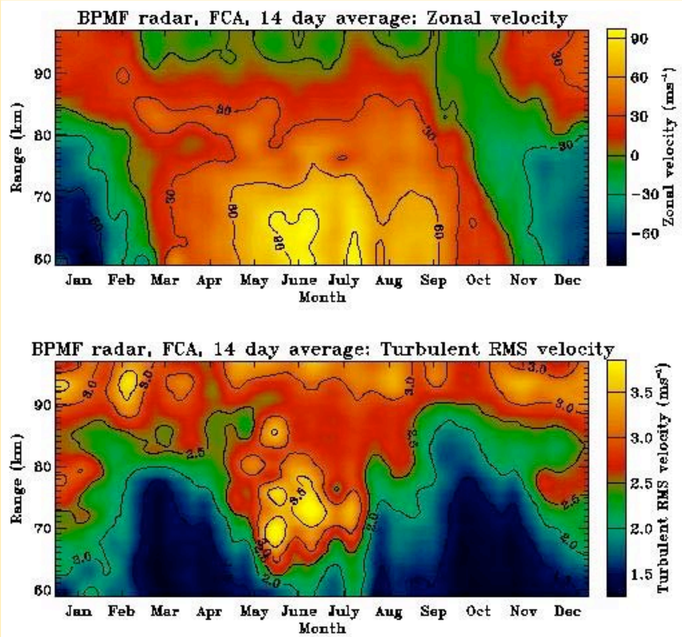

MF radar observations, Adelaide, 1999

Limitations

- Small antennas, wide beams. This means that height resolution can degrade if angular scatter is wide (> 10 deg)

- Total reflection occurs near 100 km at MF. This represents an upper limit to the technique during daytime

- Group retardation near midday causes incorrect heights to be measured above about 95 km
- Underestimation of wind speed above ~90 km

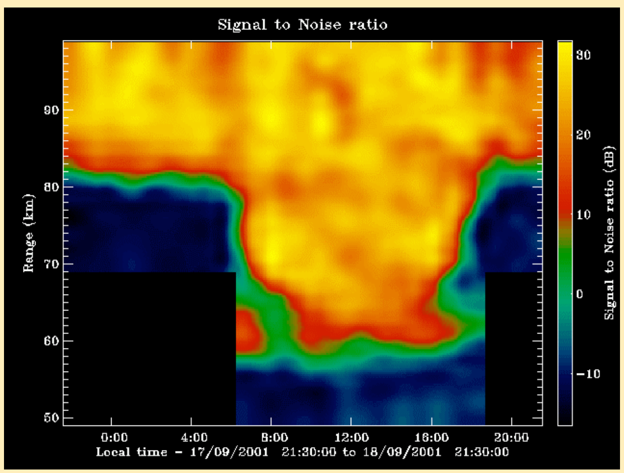

SNR 18/9/2001

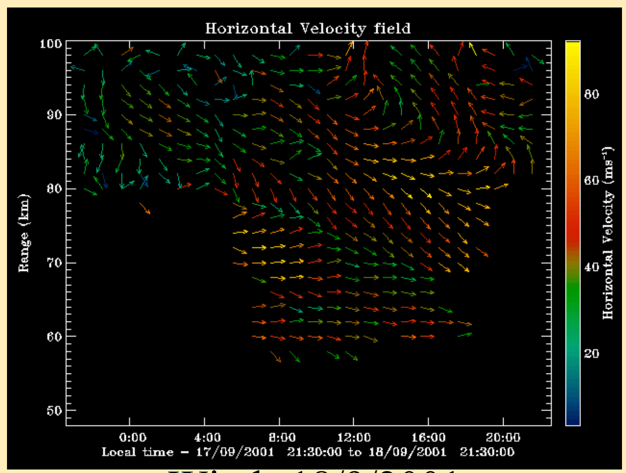

Winds 18/9/2001

Meteor Techniques I

- Frequency ~30-50 MHz
- Reflections from randomly occurring meteor trails
- Two techniques:
  - broad-beam method with interferometer to locate meteor
  - Narrow-beam radar (often ST radar)
- Line-of-sight velocities measured from Doppler shift of trail

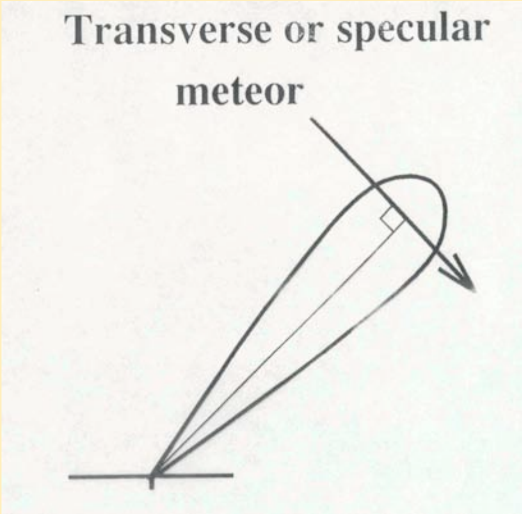

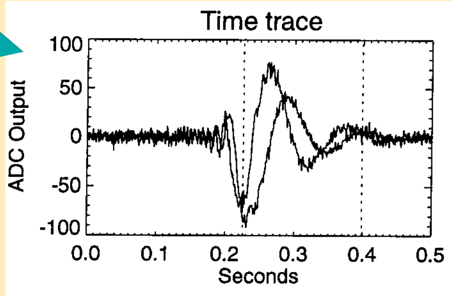

Meteors II

- Strengths
  - Reliable
  - 24-h observations
  - Continuous long-term observations for long period winds and tides
  - It is possible to infer T’/T from the diffusion of the trails
- Limitations
  - Large diurnal variation of echoes
  - Large spatial average
  - Height coverage 80 - 105 km

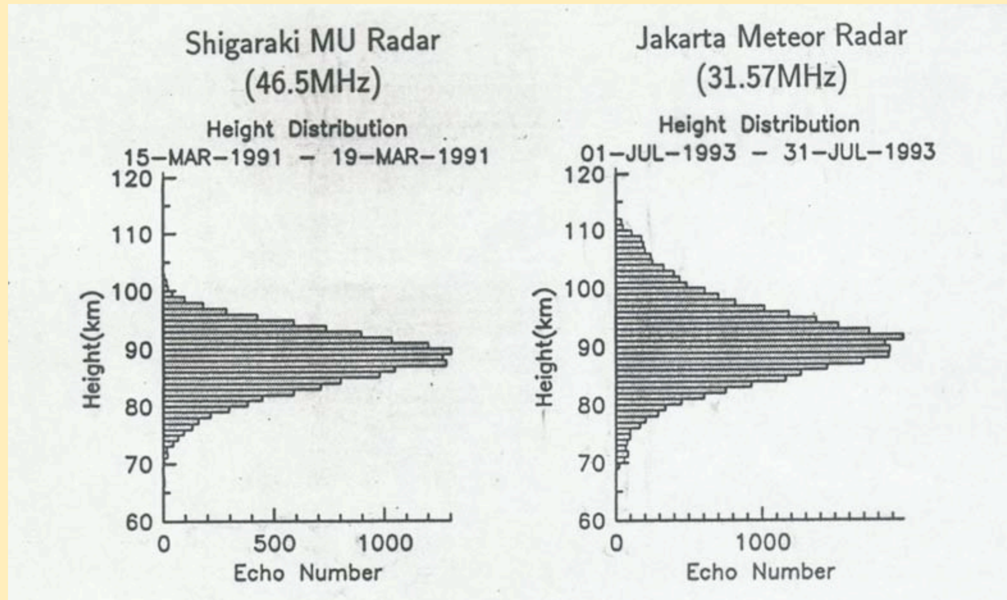

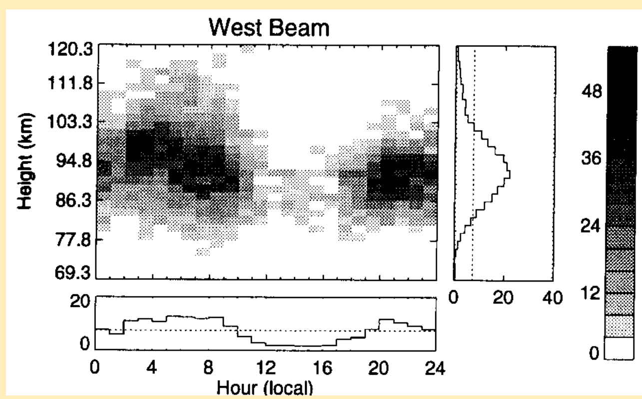

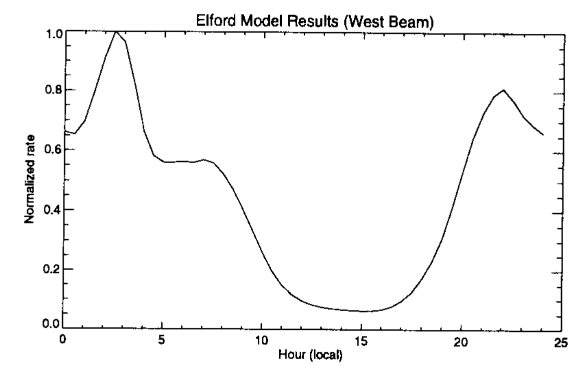

Diurnal Variation of Echoes in Space and Time

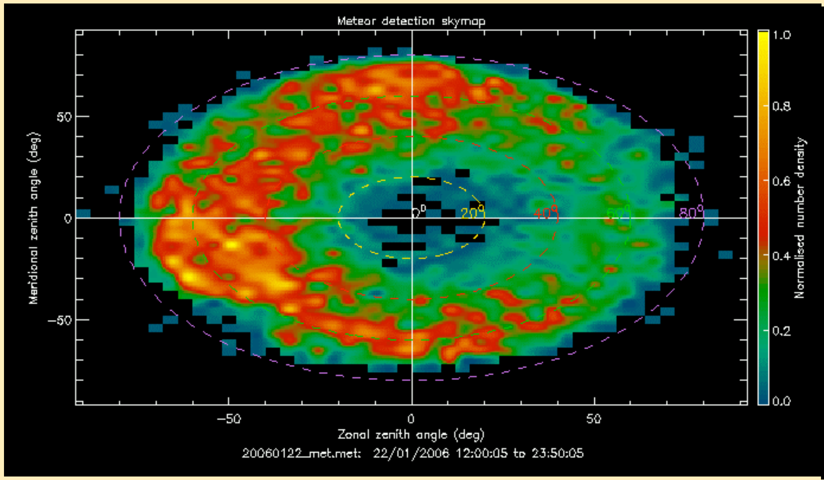

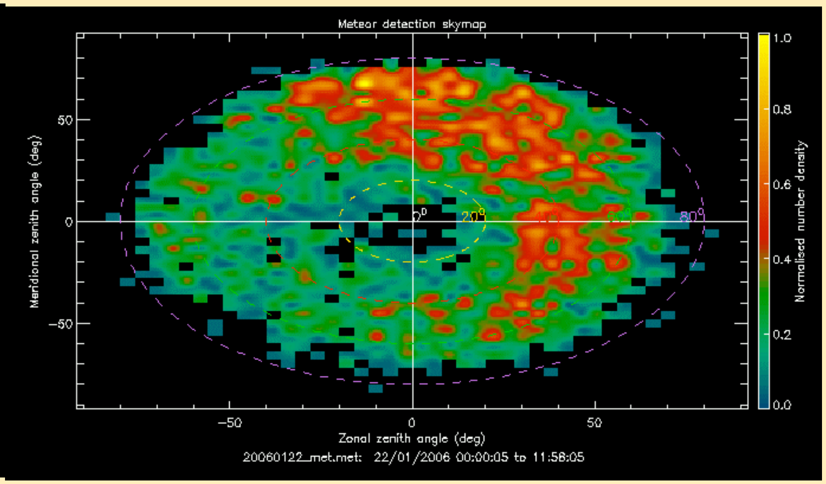

Meteor observations with an all-sky system:

- Total number of meteors/day ~3,000 - 18,000
- Note spatial variability: Morning hours (left) and evening hours (right)

CEDAR funding from NSF has supported the development and operations of lidar facilities.

Lidar Techniques

- Rayleigh-scatter lidars are a powerful tool for measuring density of neutral atmosphere
  - Vertical laser transmission
  - Telescope for reception
  - Narrow-band filter to remove unwanted light
  - Photon detection and counting
- Rayleigh scattering dominates above ~30 km, where aerosol (Mie) scattering is negligible

Types:

Rayleigh

Na wind/temp/conc.

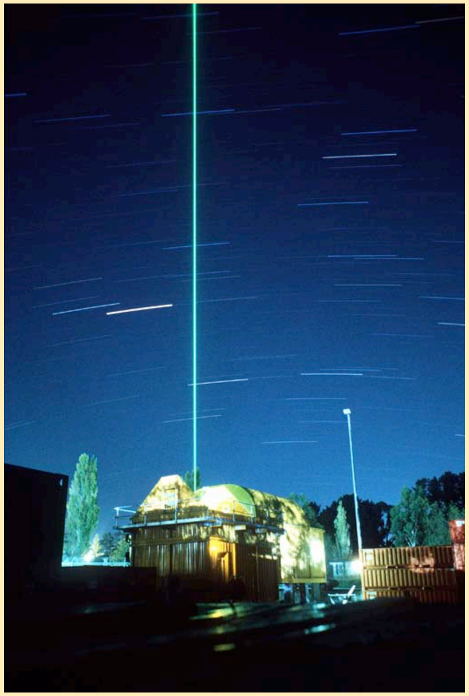

Number of photons received

Number of photons transmitted

Collecting area

Transmissivity of atmosphere

$$N(z) = \frac{N_o A \varepsilon \Im(0,z)}{4\pi z^2} n_o(z) \beta_R \Delta z$$

Pulse length

Number density of atmospheric molecules

Scattering cross-section

Lidar equation

Lidar temperature from density meas.

- •Invert lidar equation to solve for neutral density

$$\rho(z) = N(z)K\frac{z^2}{\Delta z}\Im^{-1} - n_n(z)$$

- System constant, K, usually unknown
- Need to calibrate with independent estimate of ρ.
- Usually derived from nearby radiosonde observation

Resonant scattering from sodium atoms is important technique for studying the 80-105 km region. Cross-section 10^{14} larger than for atmospheric molecules

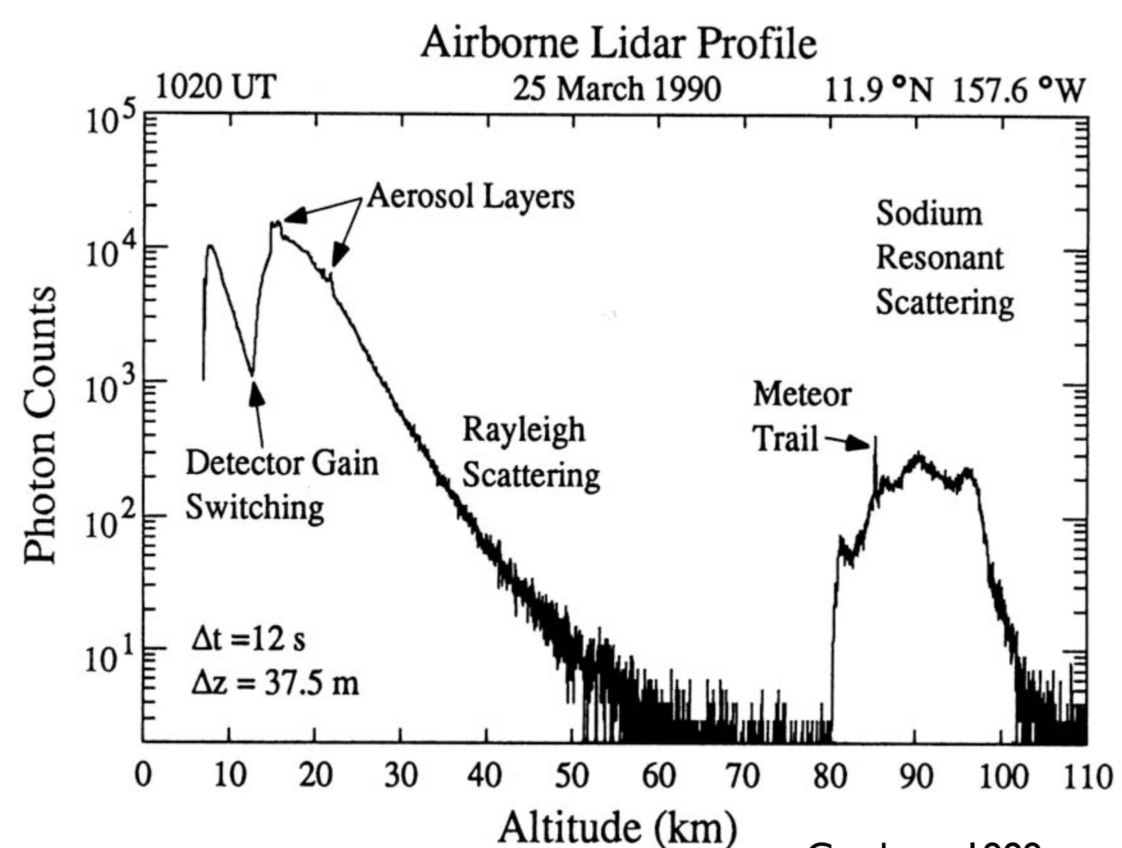

Gardner, 1989

A sodium lidar can also be used as a Rayleigh lidar but with limited range

Rayleigh Lidar Temperatures

•Convert density to temperature via equation of state and hydrostatic relation
• Make an initial guess for T_1 at *top of atmosphere* and integrate down in height (Climatology source for guess)

$$T(z) = \frac{\rho_1 T_1 + \frac{Mg}{R}\int_{z_1}^{z} \rho dz}{\rho(z)}$$

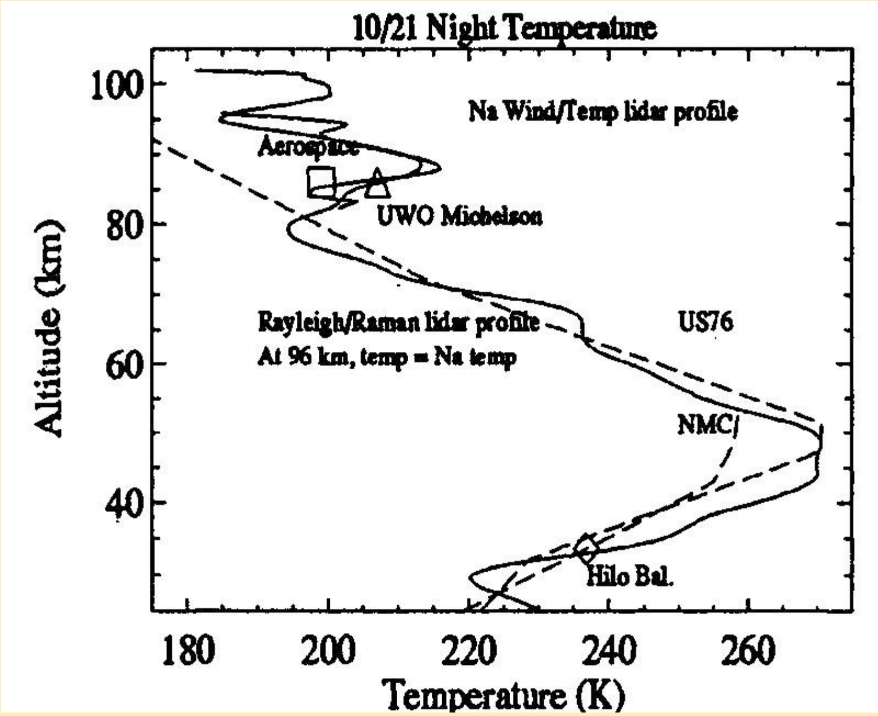

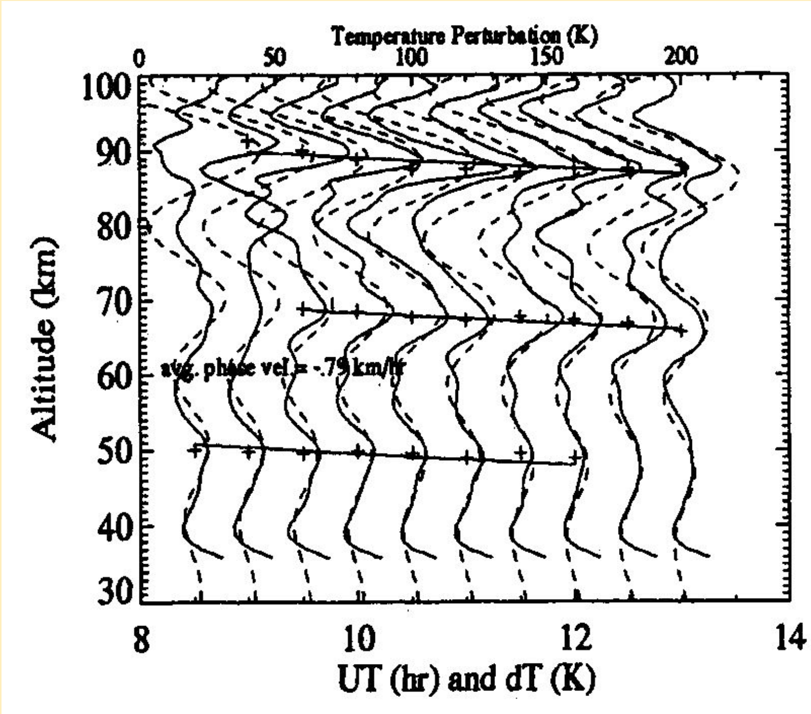

Examples from Hawaii during ALOHA-93

Na temperature lidar pioneered by She and Gardner in the early 90s

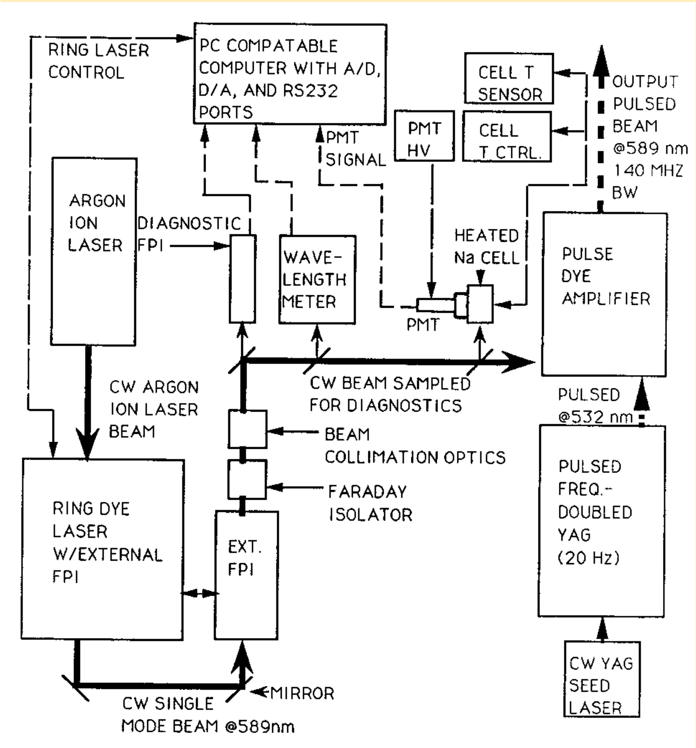

Complex transmitter, simple receiver

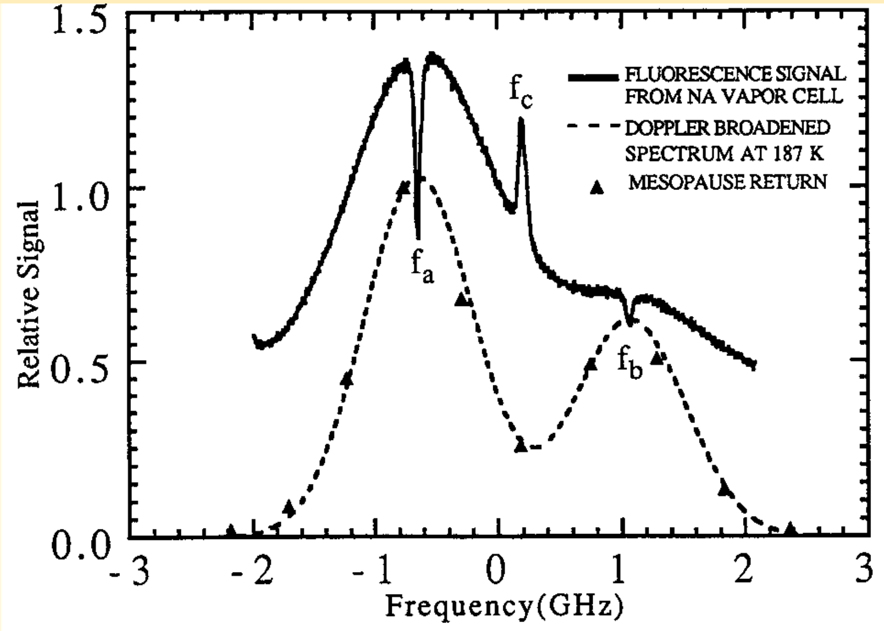

(She et al, 1990)

Doppler free spectroscopy is used to determine T(h) by evaluating ratio of fa and fb intensities.

- Comparison of UARS winds with several MF radar data sets showed significant discrepancies that were attributed by Burrage et al.[1994] to difficulties in MF analysis algorithms. UARS HRDI data were validated by comparison with WINDI, with rocket data, and with results from several meteor radar systems.

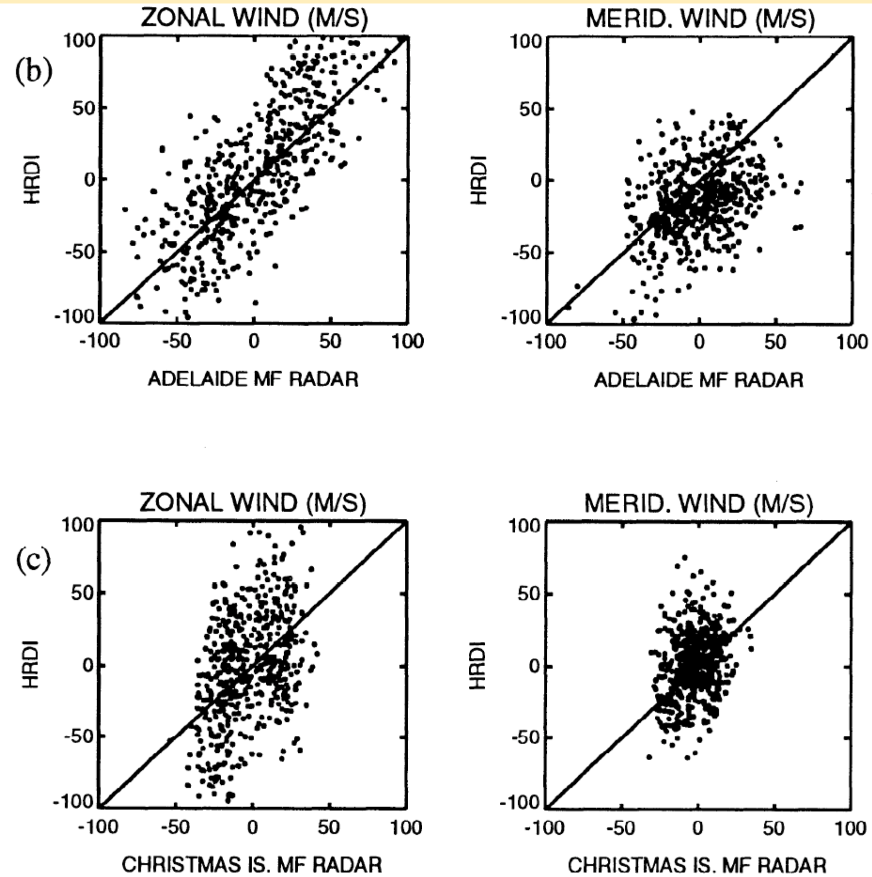

Figure 11. Scatterplots of HRDI winds in the altitude range 65-85 km for the zonal and the meridional components using (a) 106 coincidences with the Urbana MF radar between December 1991 and December 1993, (b) 118 coincidences with the Adelaide MF radar between December 1991 and January 1994, and (c) 137 coincidences with the Christmas Island MF radar between December 1991 and January 1994.

How do lidar and meteor radar winds compare?

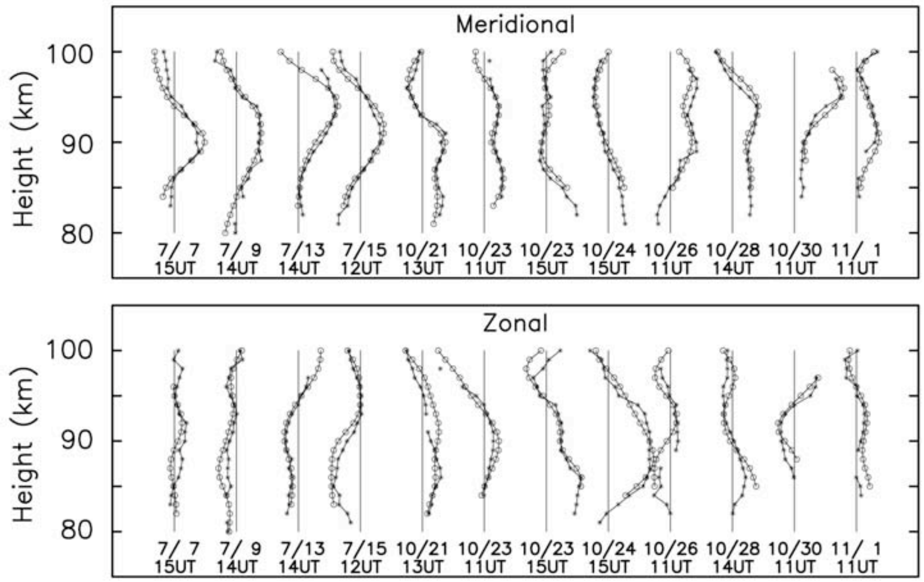

Figure 1. Sample (top) meridional and (bottom) zonal wind profiles collected during the July 2002 and October 2003 campaigns. Lidar profiles are marked with circles, and radar profiles are marked with asterisks. The profiles are scaled such that the horizontal distance between vertical lines corresponds to 150 m/s.

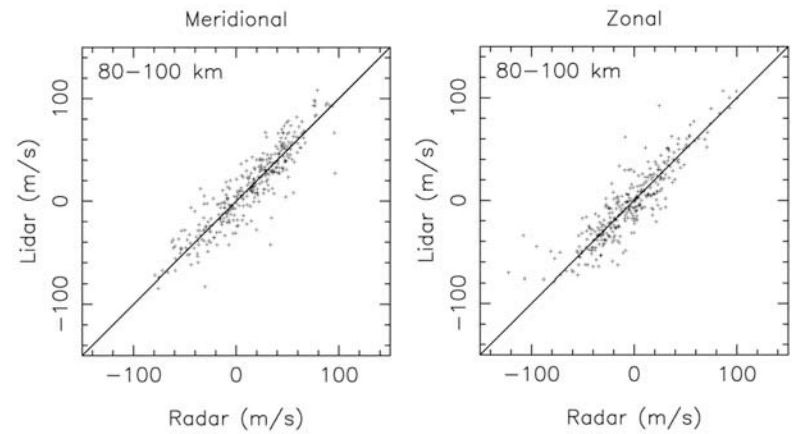

Figure 2. Scatterplots for all coincident radar and lidar measurements in 80–100 km altitude range.

Franke et al., 2003

Answer: Pretty well. Comparison of Maui lidar winds for two separate periods after application of height and time averaging to match meteor radar measurements (4 km, 1 hr)

Radar not able to observe shear region seen by lidar as not able to observe with the necessary vertical spatial resolution.

Airglow Imagers

- Optical techniques allow direct imaging of airglow layers

  OH ~87 km

  O_2 atmospheric ~93 km

  O(^{1}S) 557.7 nm ~97 km

- Emissions focussed on CCD detector through narrow-band filter
- Study small-scale structure of atmosphere
- Temperatures can be measured by comparing line strengths in OH, O_2 bands

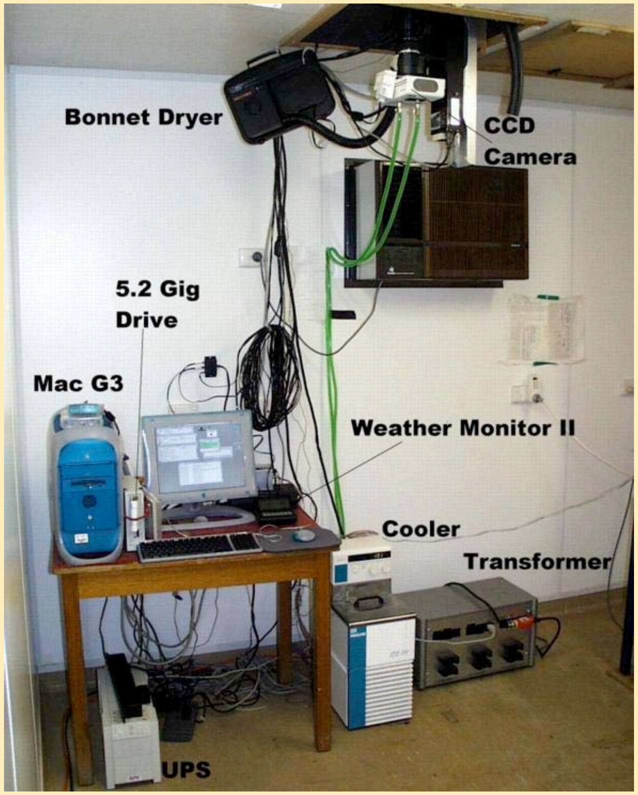

The Clemson airglow imager

Imaging examples

- All-sky imagers provide excellent documentation of the dynamic behavior of the nightglow or aurora.
- Very useful for dynamical studies of waves within the mesosphere region.
- Change filters to capture image of nightglow at different altitude

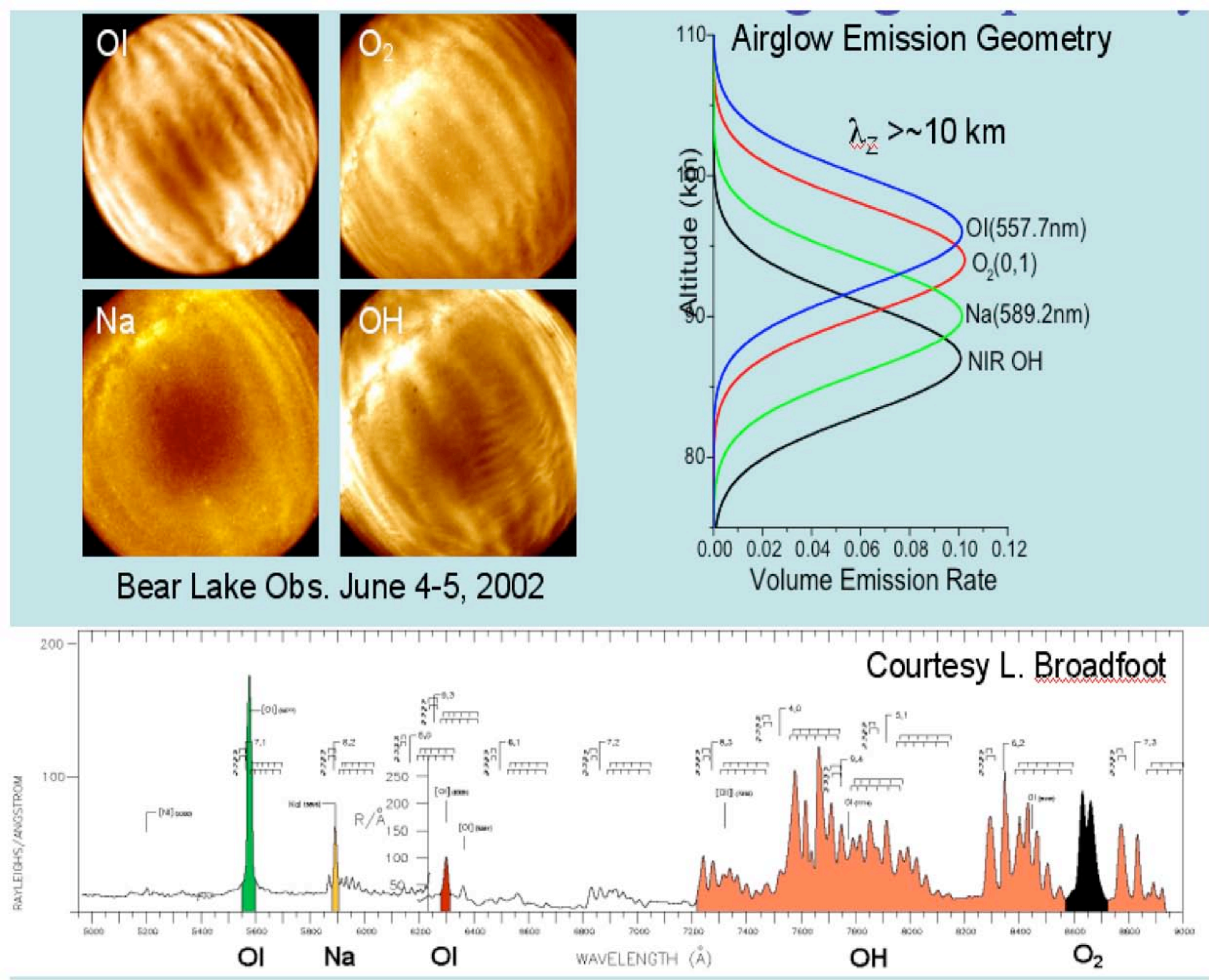

Courtesy, M. Taylor

Overview of Airglow Phenomena

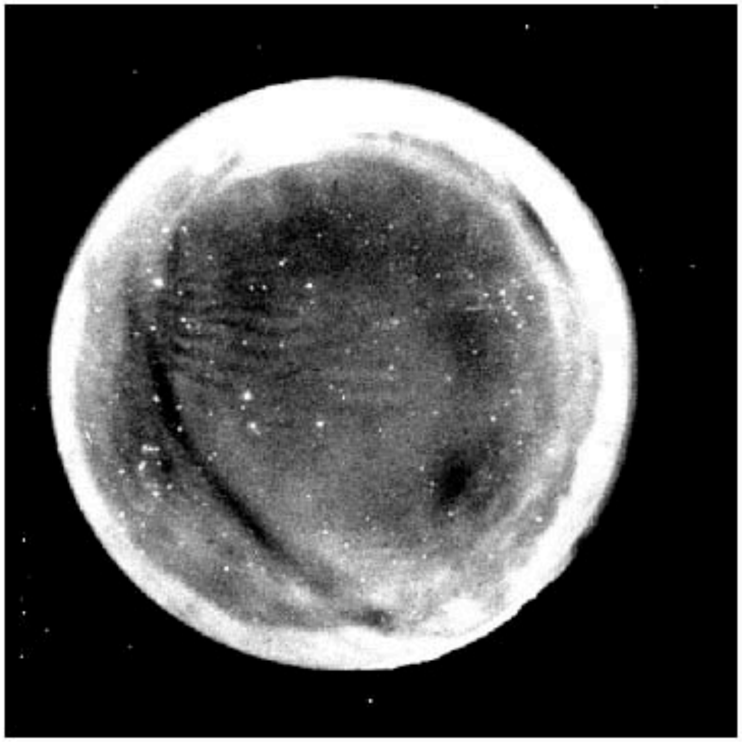

3:50 October 15, 2001

- The dark line in the bottom-left corner is an example of a rare phenomenon called a "bore"
- There also appear to be wave-like structures in the center, towards the bore. This is a more common phenomenon, called ripples
- The stars can be used to calibrate the image spatial scale and to determine the cardinal directions (N, E,S,W)

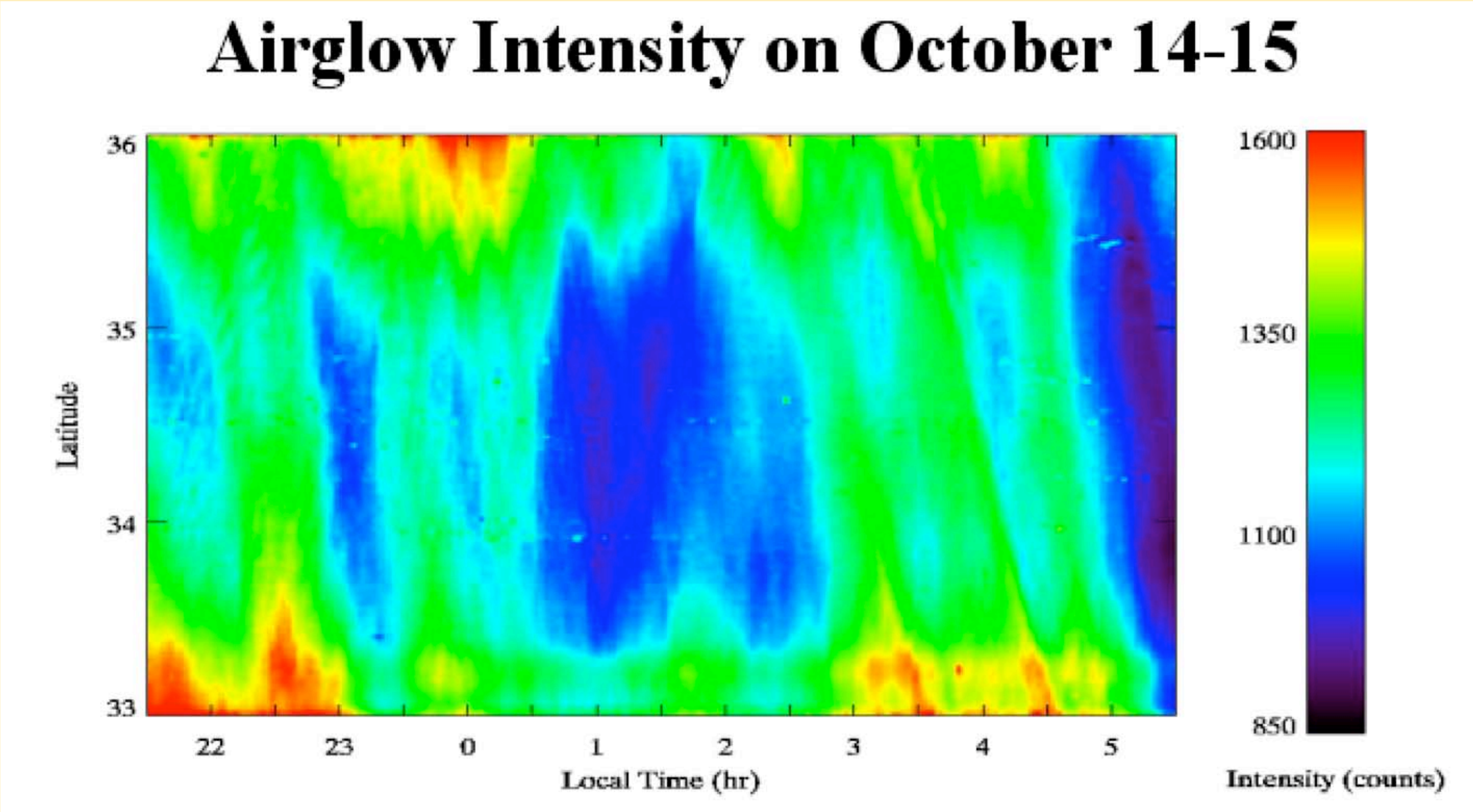

The keogram is a useful way of portraying imaging observations

- The optical imaging community has made valuable contributions to the study of:
  - Heating experiments

Bernhardt et al., 1999

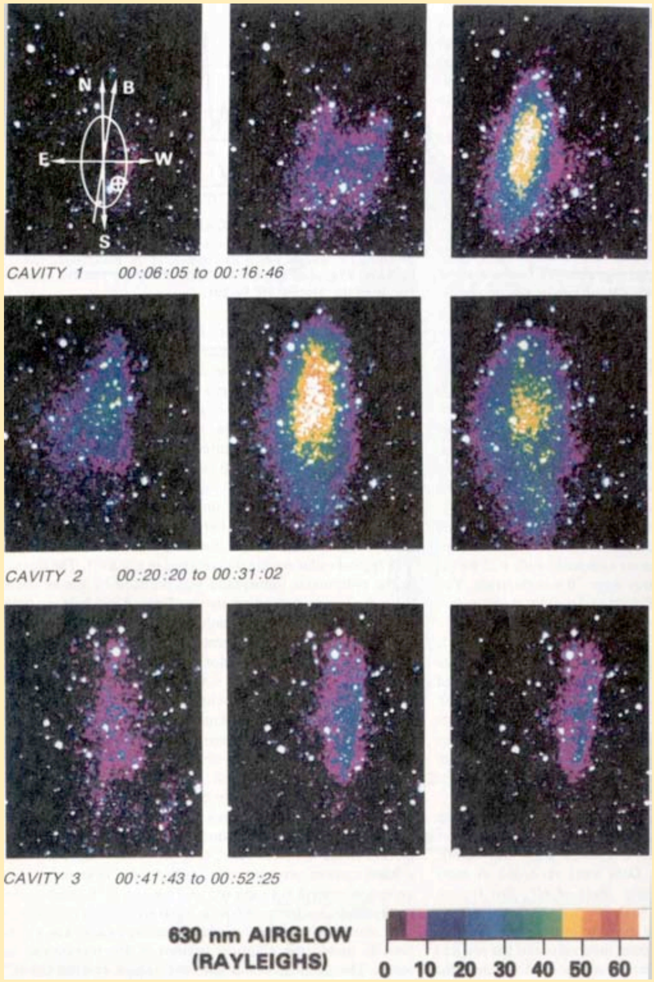

White light imagers at high latitudes

- **Extensive arrays exist at high-latitudes to study auroral processes**
  - Time History of Events and Macroscale Interactions during Substorms (THEMIS)
  - Magnetometers-Ionospheric Radars-Allsky Cameras Large Experiment (MIRACLE)

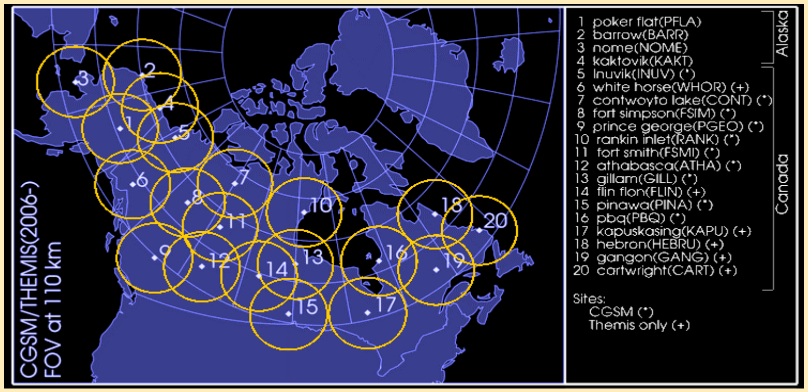

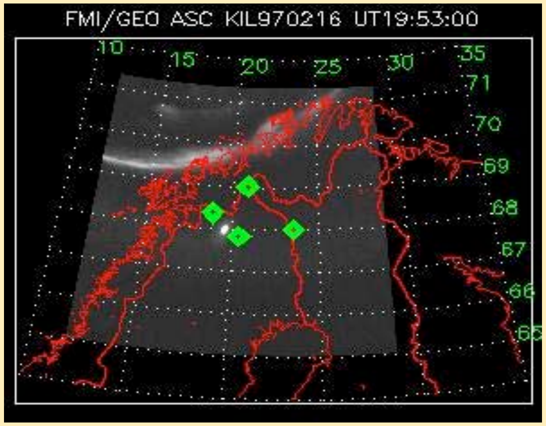

Satellite Remote Sounding Techniques

- Example: HRDI Limb-viewing Fabry-Perot instrument
- Measures Doppler shift of airglow emission and absorption lines
- Two views of same volume at 90° to UARS gives velocity
- Vertical resolution ~2-3 km
- ~60-120 km (MLT mode)
- ~10-40 km (stratospheric mode)

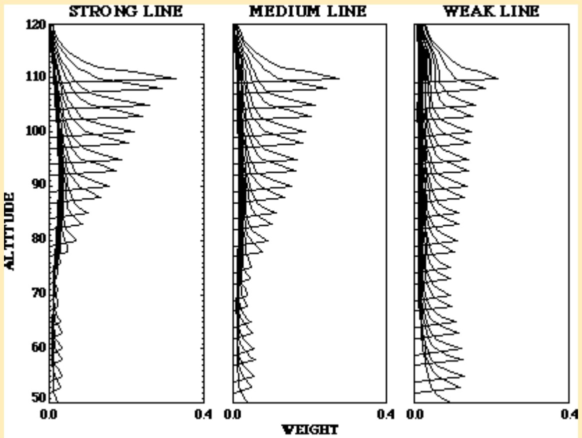

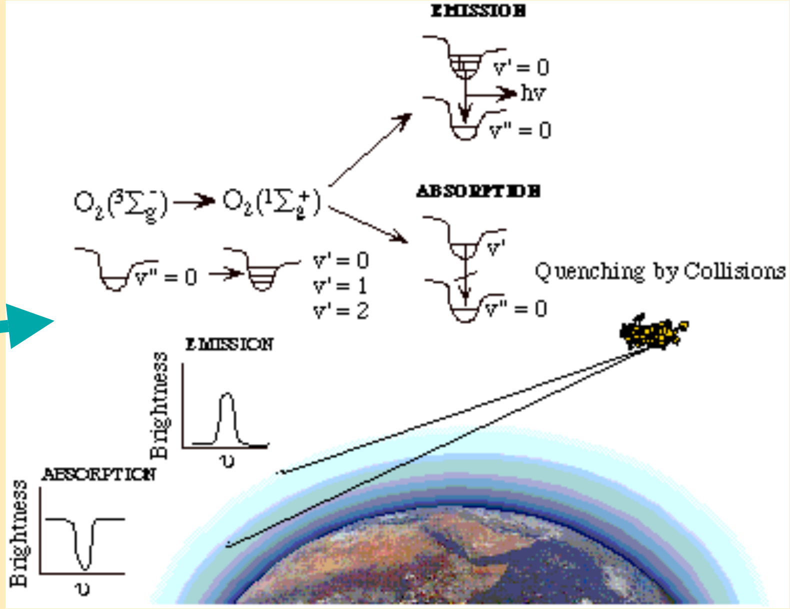

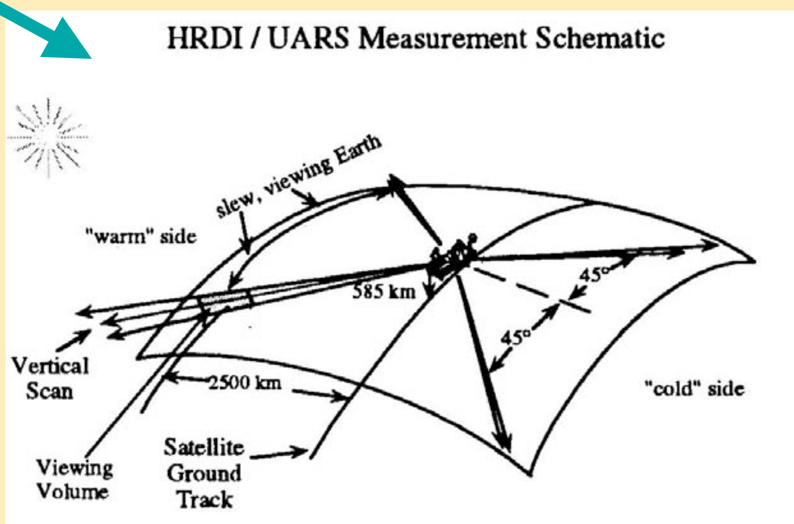

HRDI Winds

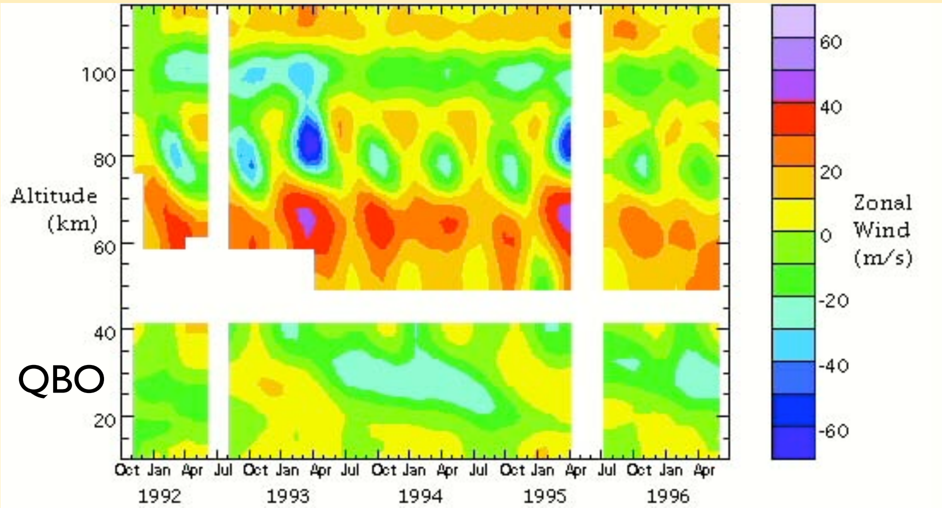

QBO

Monthly-mean zonal winds

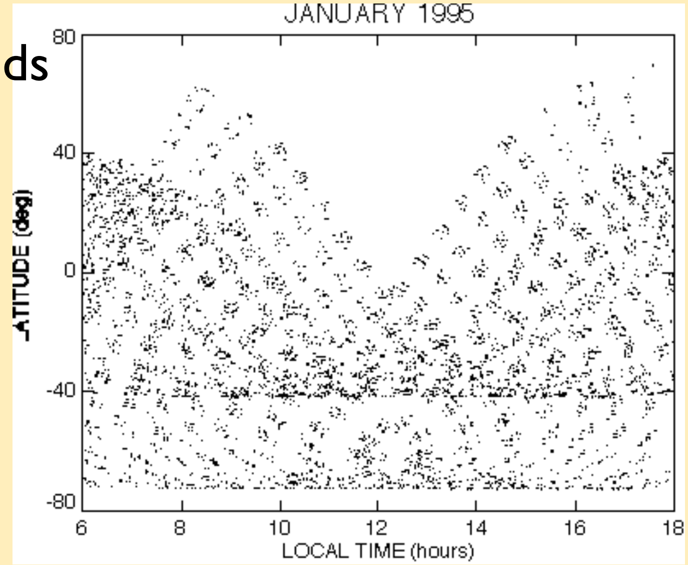

- **Strengths**
  - Global coverage
  - Large height range
  - Good height resolution
- **Weaknesses**
  - Limb-viewing means horizontal resolution ~200 km
  - Slow precession of UARS/TIMED limits latitudinal coverage
  - Limited local time coverage

Local time coverage as a function of latitude for January 1995.

GPS Occultation Techniques

- Low-Earth orbit (LEO) satellite monitors L1, L2 transmissions from GPS satellites
- L1 (L2) = 1.6 (1.2) GHz
- Signals strongly refracted as GPS satellite is occulted by atmosphere and ionosphere

- Signal delays converted to $\rho(z)$ after removal of ionospheric (dispersive) refraction
- Temperature profiles derived using hydrostatic equation
- Humidity profiles if pressure known at surface

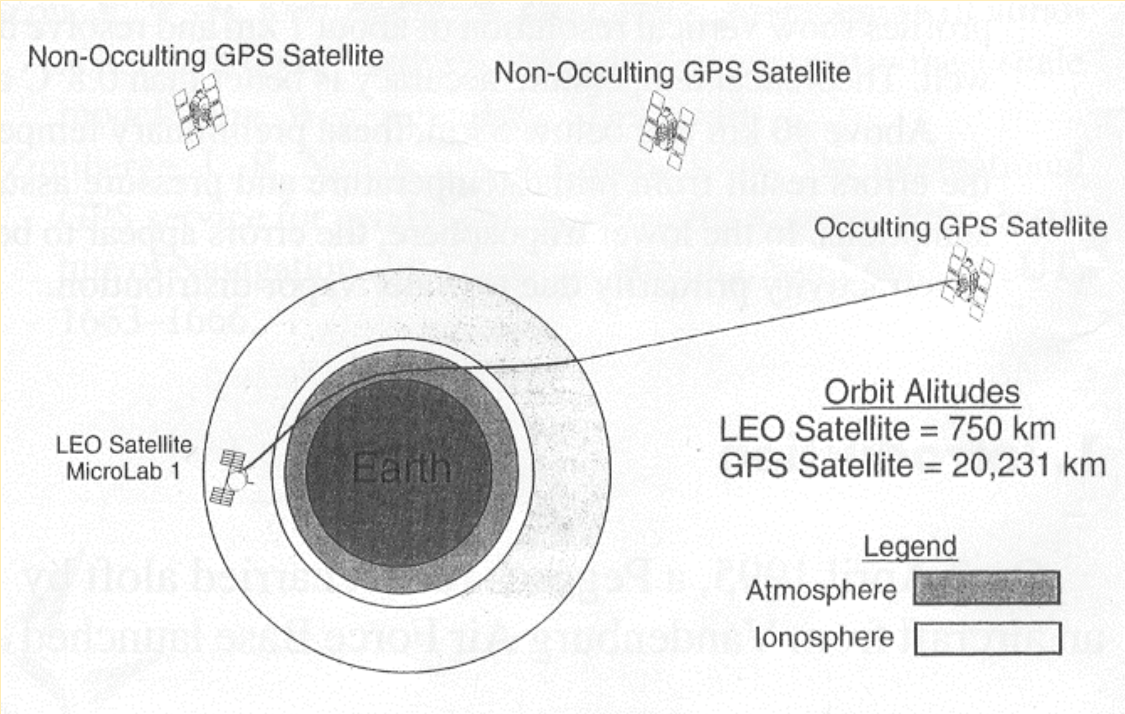

GPS II

- Strengths
  - Global coverage
  - "Inexpensive" LEO satellites
  - N_e, T, e profiles and climatologies
  - Moderate height resolution (~1-2 km)
- Weaknesses
  - ~200-300 km horizontal resolution

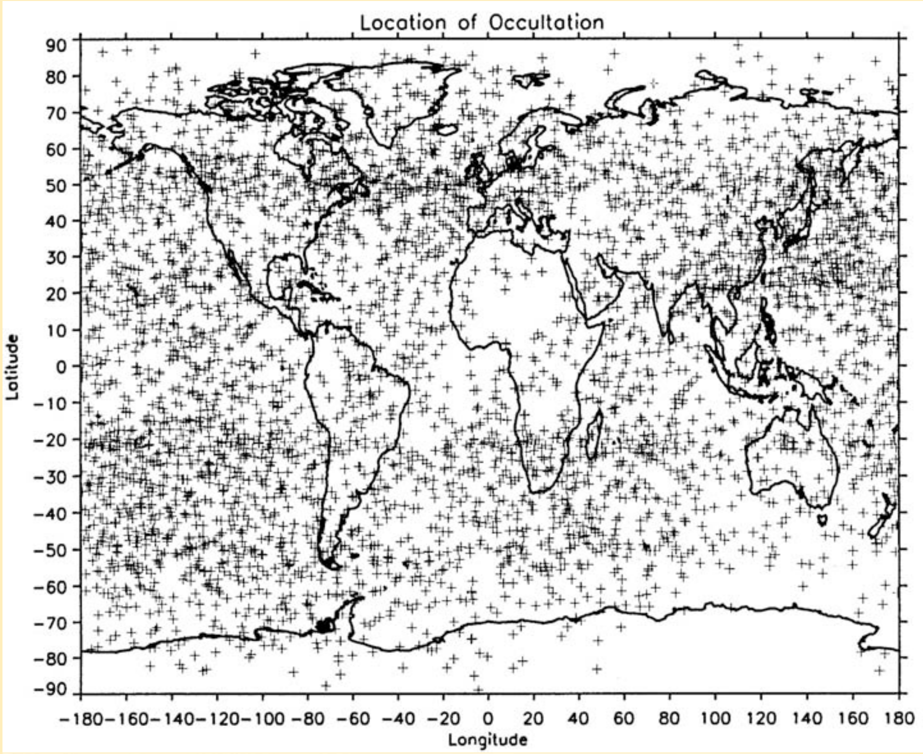

GPS/MET Occultations Nov 96-Feb 97

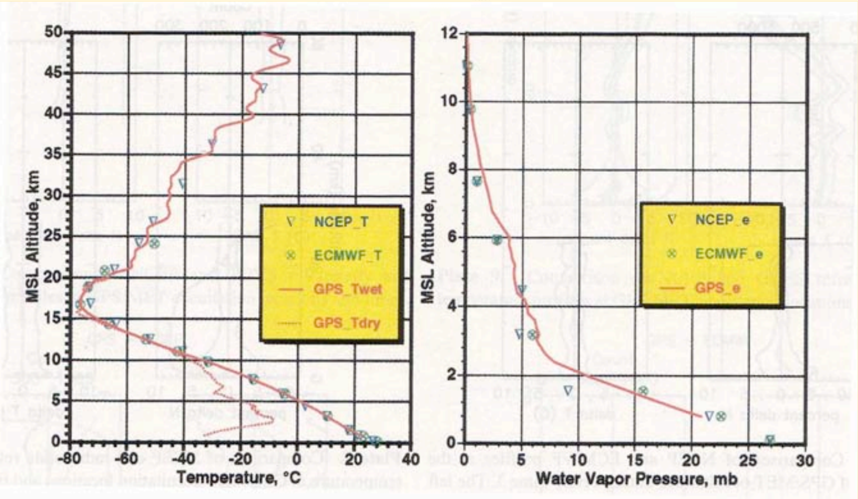

Validation

Where does it all begin?

Sun-Earth System: Energy Coupling

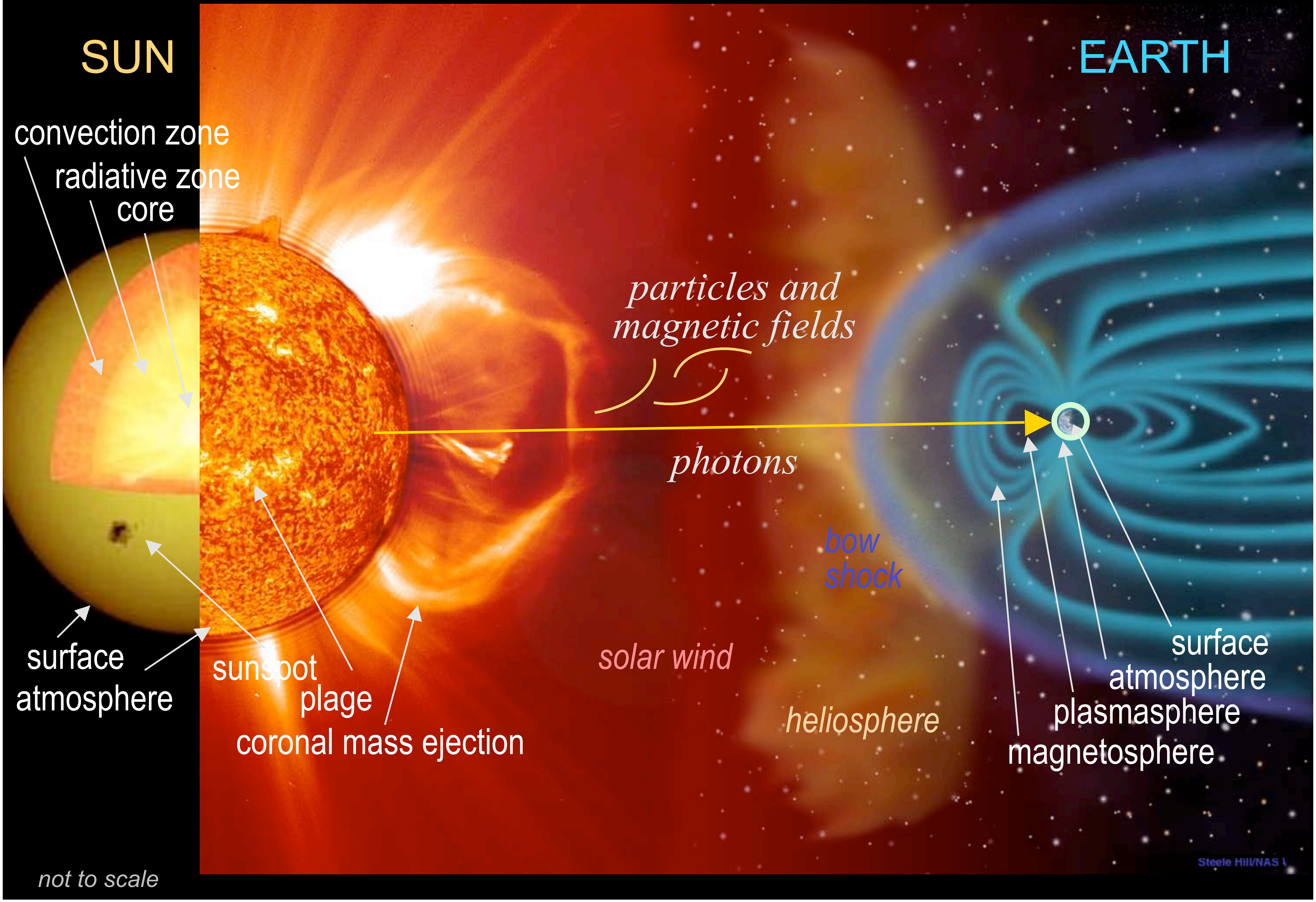

Why does the Atmospheric Temperature vary with Altitude?

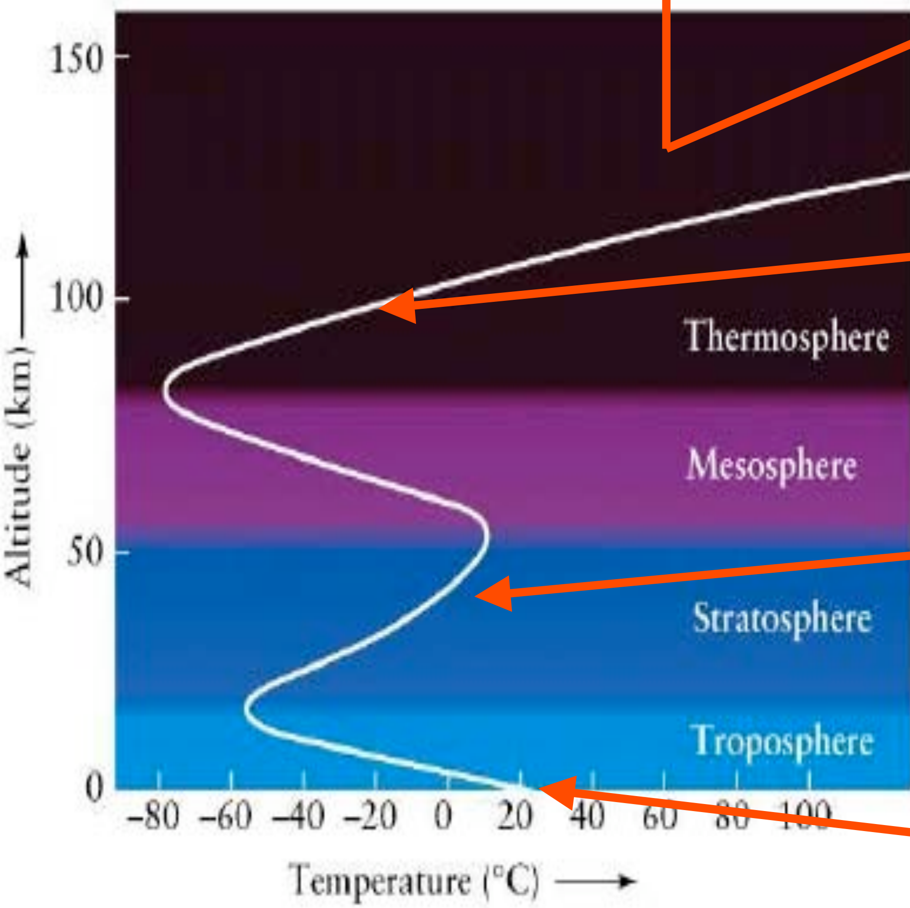

Ionization:
O, N_2, O_2 + sunlight → e + …

Oxygen Heating:
O_2 + sunlight → O + O

Ozone Heating:
O_3 + sunlight → O + O_2

Surface Heating

Thermal Structure of Mesopause Region

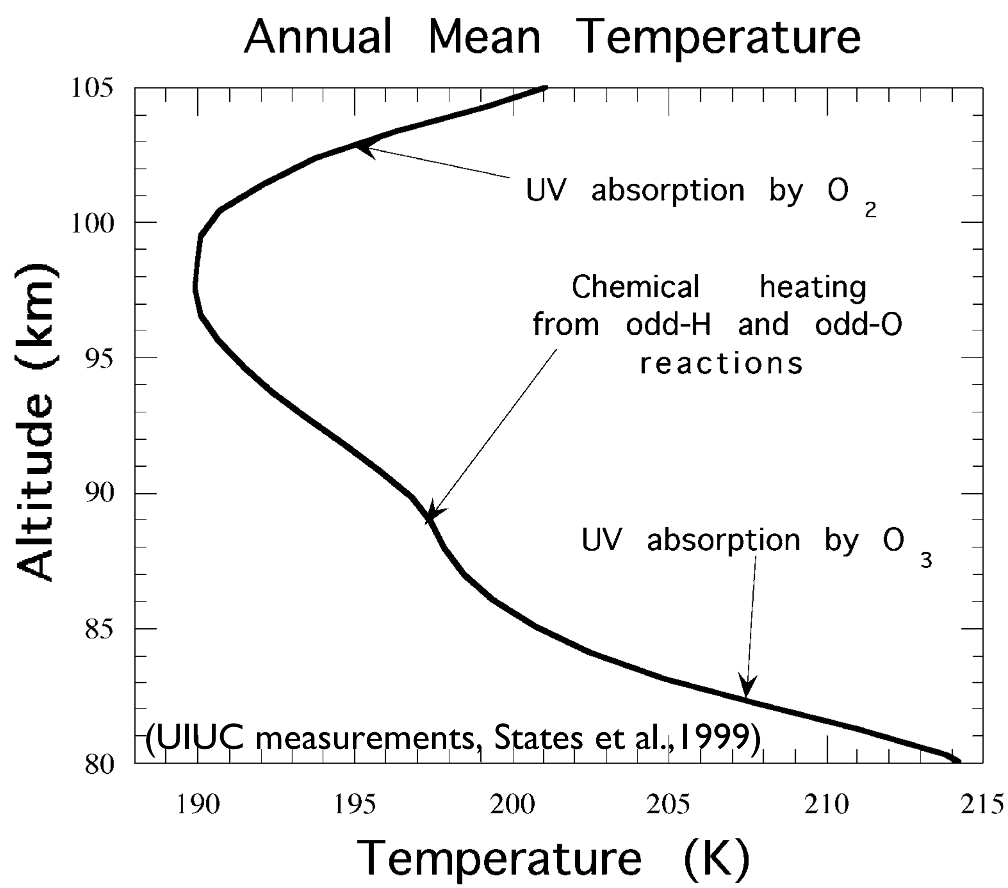

Schuman-Runge Bands & Continuum 135-200 nm

Lyman-a line 121.5 nm

Hartley Band 200-300 nm

IR Radiative Cooling By CO_2 (15µm)

Illinois observations show chemical heating as relatively weak source

The Two Atmospheres

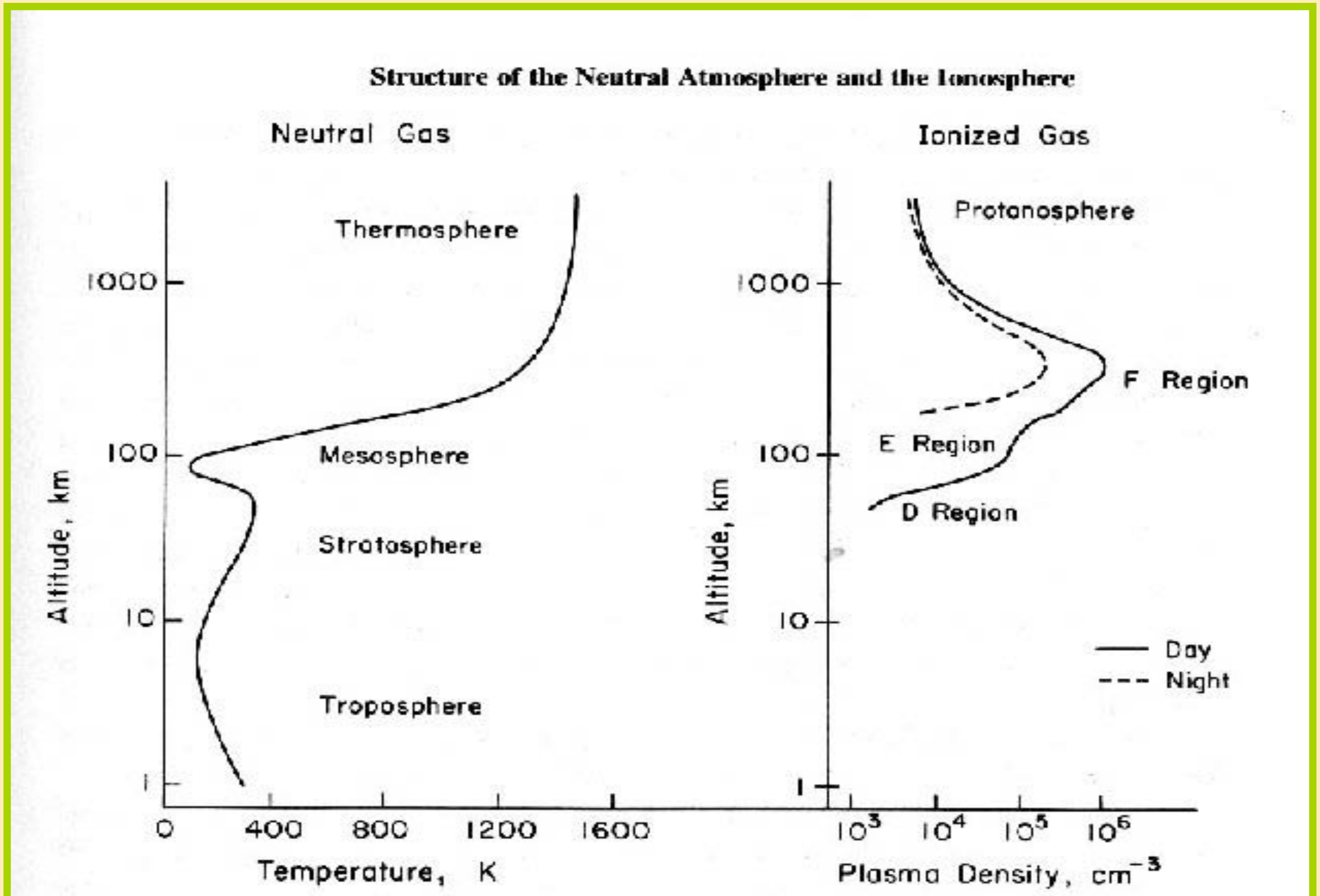

Solar Radiation Absorption

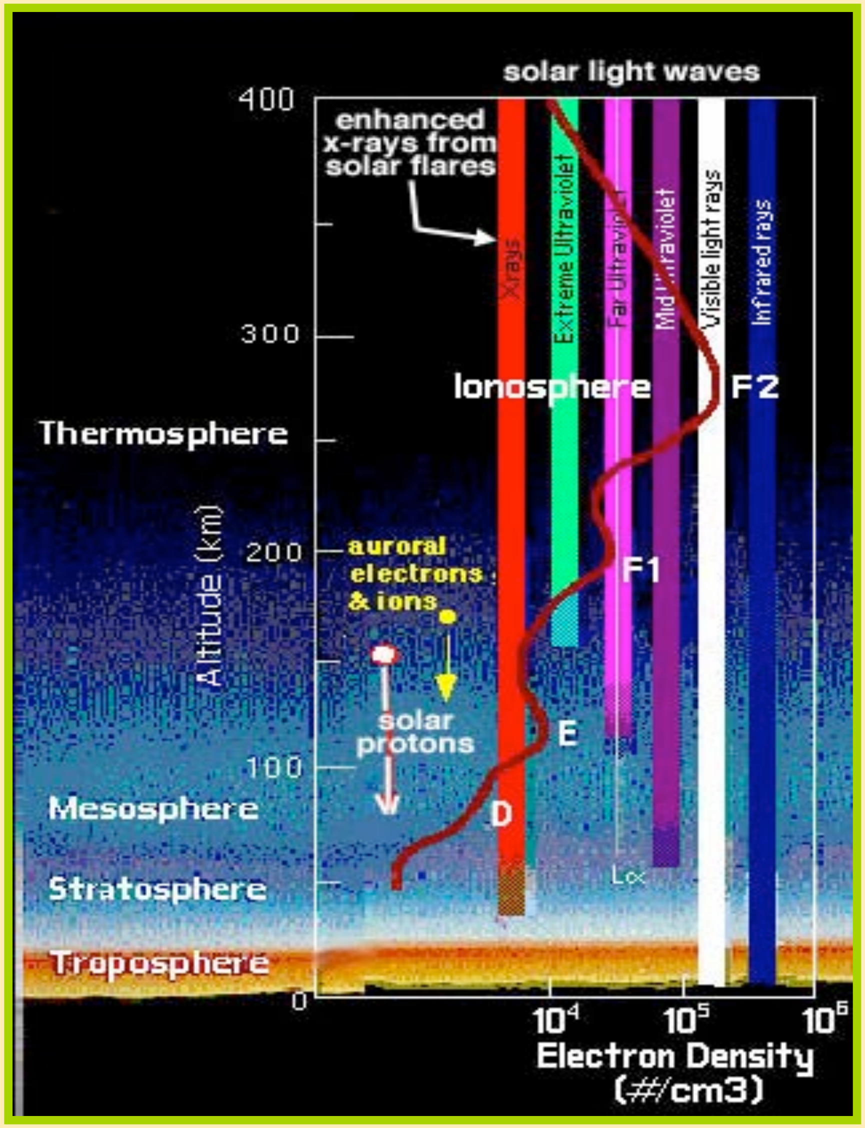

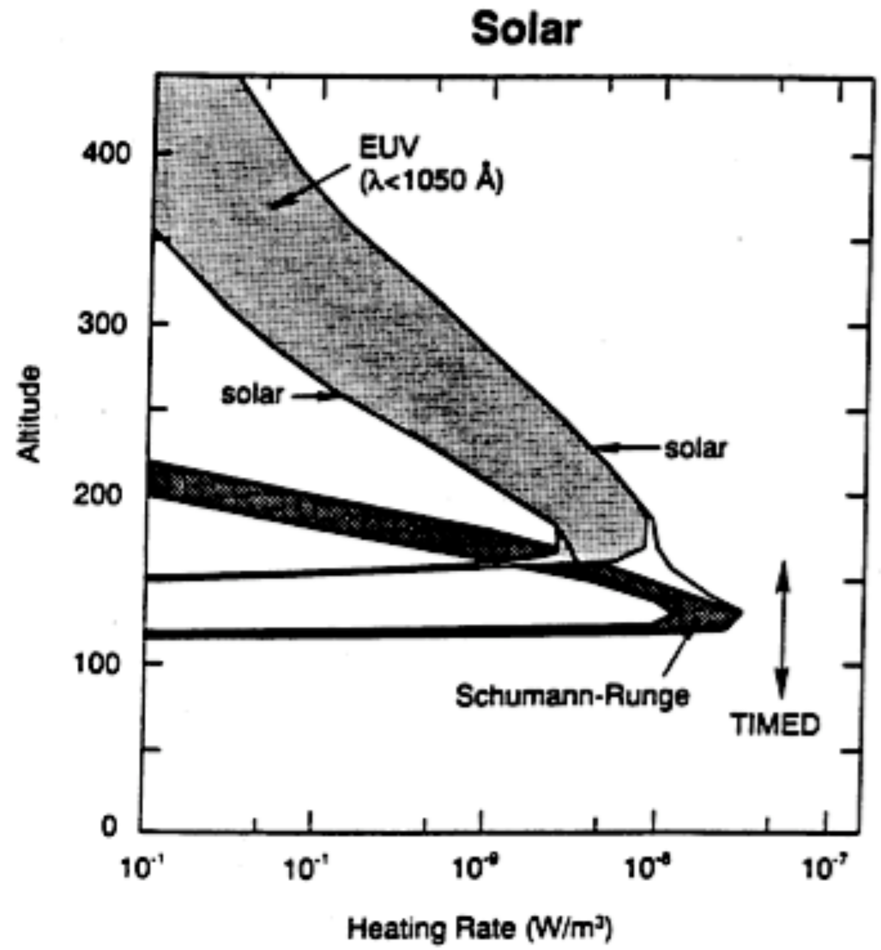

Altitudinal profiles of heating rates due to solar EUV and UV absorption. The shaded regions indicate the range of variations with solar activity. The TIMED Mission investigates the region of maximum energy deposition.

EUV portion of solar spectrum particularly variable

Solar cycle changes in EUV radiation impact upper atmosphere temperature and density

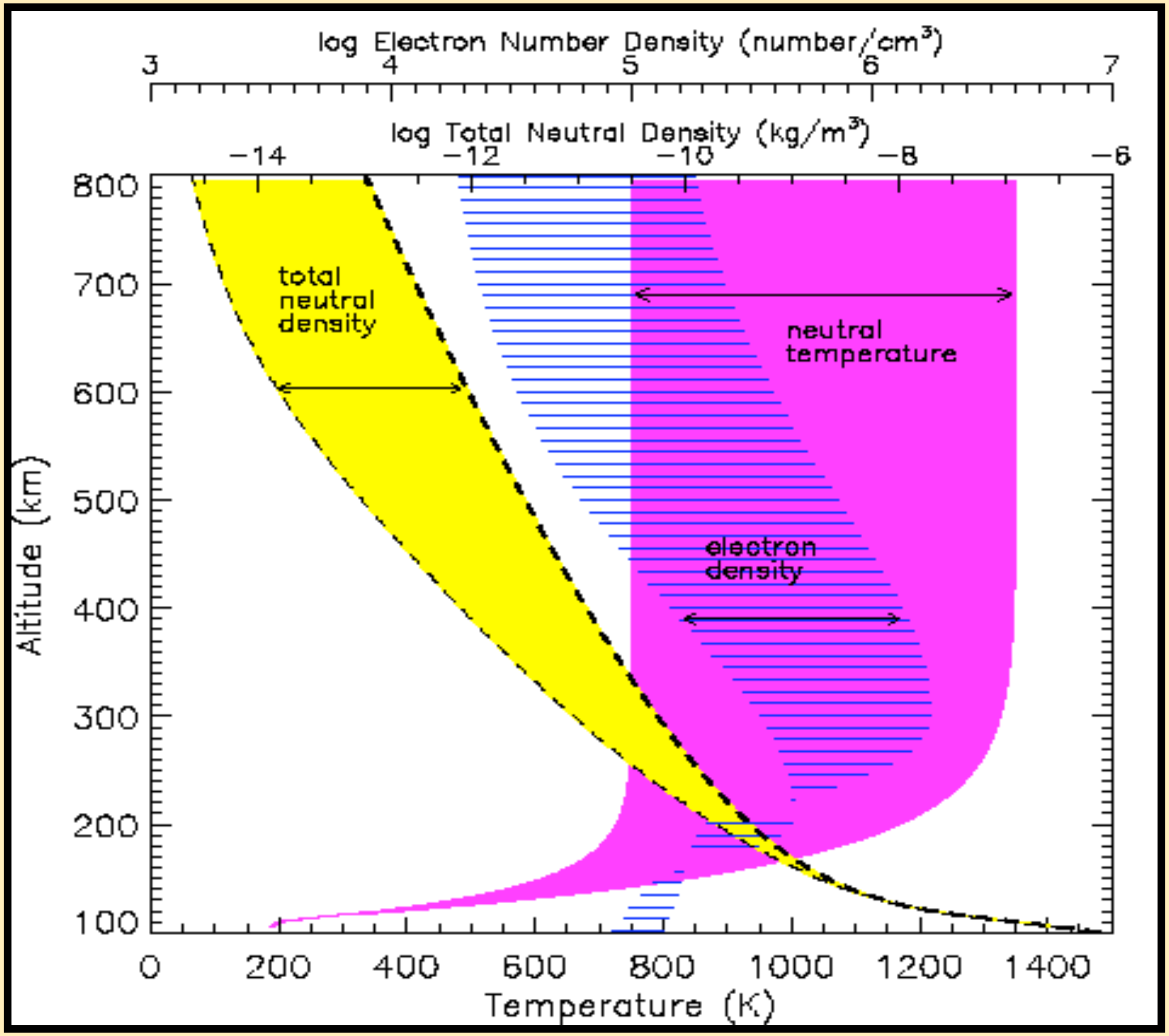

Solar Cycle Changes at 700 km:

Neutral Temperature: 2 times

Neutral Density: 50 times

Electron Density: 10 times

Solar Energy in the Upper Atmosphere

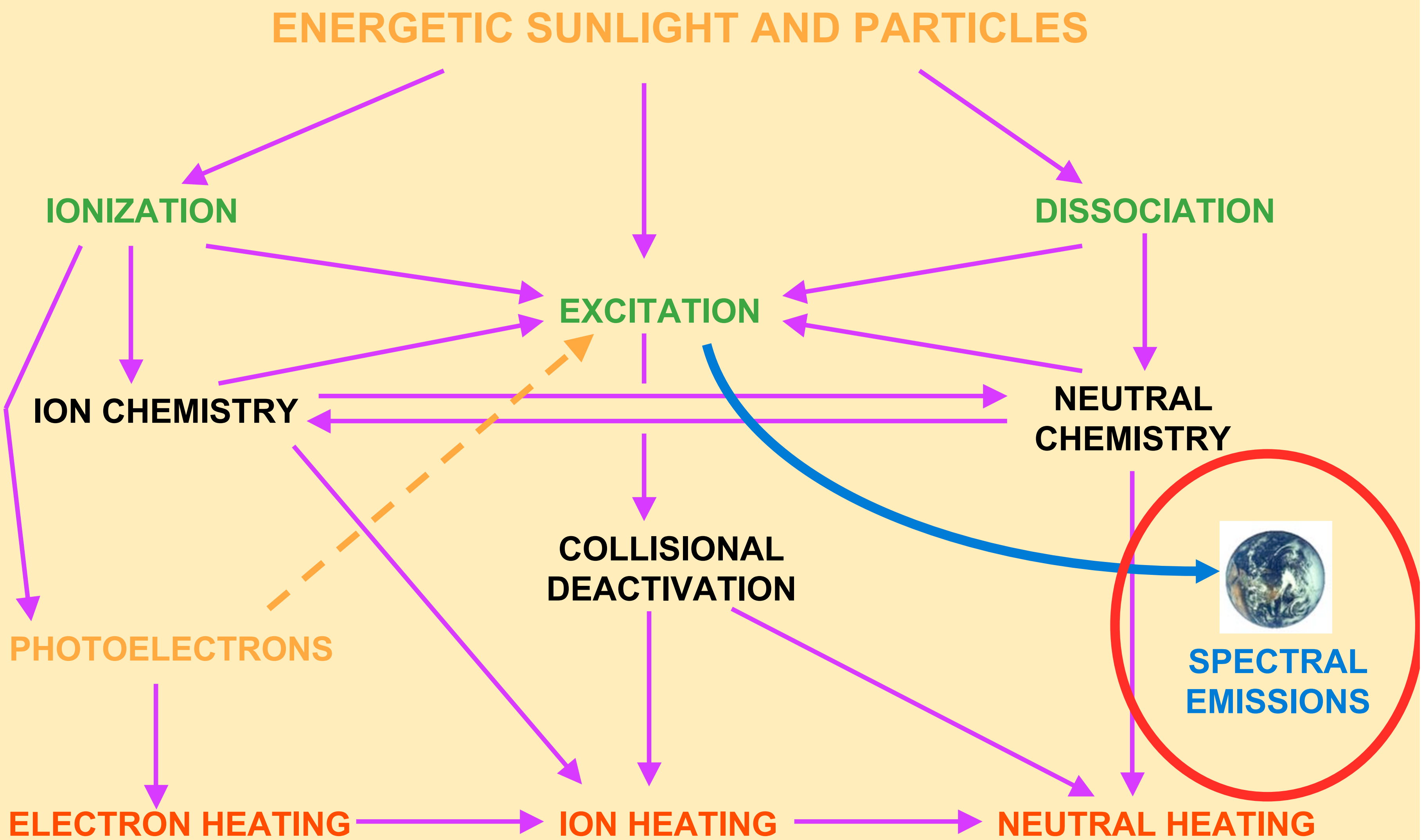

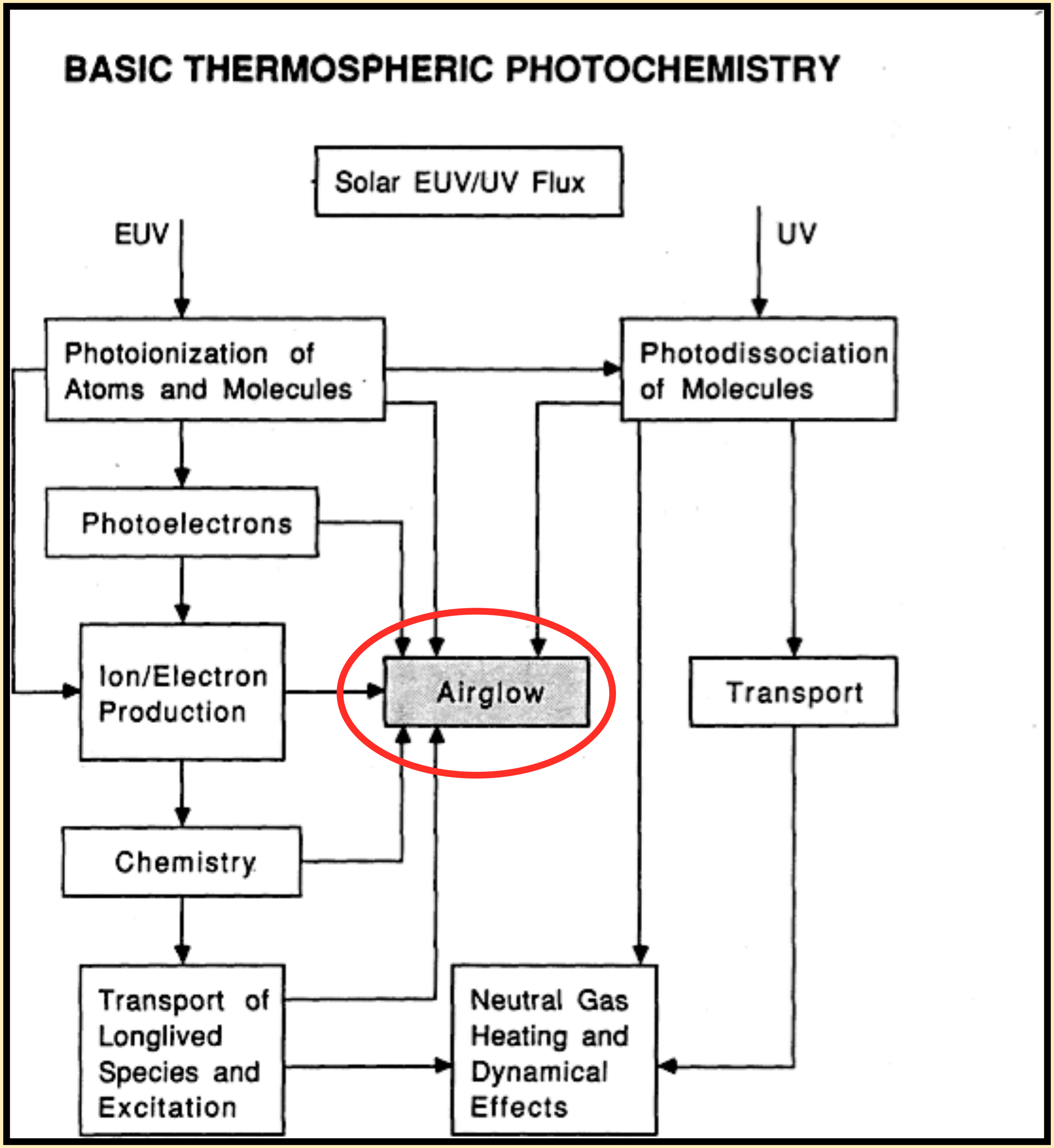
BASIC THERMOSPHERIC PHOTOCHEMISTRY
Solar EUV/UV Flux
EUV
UV
Photoionization of Atoms and Molecules
Photodissociation of Molecules
Photoelectrons
Ion/Electron Production
Airglow
Transport
Chemistry
Transport of Longlived Species and Excitation
Neutral Gas Heating and Dynamical Effects

Photochemical systems (complicated!)

- Major species (O,O_2,N_2)
- Reservoir molecules (H_20,H_2)
- Metastable neutrals
- Permitted excited states
- Odd hydrogen family
- Odd oxygen family
- Odd nitrogen family
- Metallic neutrals and ions
- Major and minor ionic species
- Metastable ions
- Cluster ions
- Tracer species

MESOSPHERE LOWER THERMOSPHERE PHOTOCHEMICAL SYSTEMS

SYSTEM	MEMBERS	REGION	ROLE
MAJOR SPECIES	O, O_2, N_2	MLTI	ENERGY ABSORBERS, REACTANTS START OF PHOTOCHEMICAL CHAIN
METASTABLE NEUTRALS	$O(^1D)$, $O(^1S)$, $N(^2D)$, $N(^2P)$	MLT	ENERGY STORAGE/TRANSFER
	$N(^2P)$, $N_2^*(V)$, $O_2^*(V)$, $N(^2A)$		KINETICS MODERATORS
	O_2(A, A' ,C1 , a, b), OH^*		RADIATORS/HEAT LOSS
	CO_2(VIB)		OBSERVABLES
EXCITED STATES	O, O_2, N_2, N, OH, NO		RADIATORS/HEAT LOSS
			METASTABLE SOURCES
ODD OXYGEN (Ox)	O	M	SINGLE SOURCE OF O_3
			KEY REACTANT
			RADIATOR/HEAT SINK
			CHEMICAL HEAT SOURCE
	O_3	M, STRAT	UV ENERGY ABSORBER, RADIATOR, REACTANT
			CLIMATOLOGY CONTROL
			D REGION ION CHEMISTRY
ODD HYDROGEN	H, OH, HO_2, (HOx)	M	CATALYTIC Ox DESTRUCTION
			CHEMICAL HEAT SOURCES
HOx RESERVOIRS	H_2O, H_2		HOx PHOTOCHEMICAL SOURCES
ODD NITROGEN	N, $N(^2D)$, $N(^4S)$, NO, NO_2	LT	HEAT SOURCES AND TRANSFER, REACTANTS
	$N(^2D)$	LT	OBSERVABLE FOR NO^+
	NO	LT	SOURCE OF NO^+
		MLT	RADIATOR/HEAT SINK
		MLT	SOURCE OF STRAT NO
		STRAT	O_3 CATALYTIC DESTRUCTION
METALLIC NEUTRALS	Na, Ca, K, Fe	M	OBSERVABLES/TRACERS
MAJOR IONS	O^+, O_2^+, NO^+, N_2^+	MLTI	REACTANTS/HEAT SOURCES
MINOR IONS	N^+	LT	MINOR REACTANT
METASTABLE IONS	$O^+(^2D)$	LT	CHEMICAL ENERGY TRANSFER
	$O^+(^2P)$	T	LT COMPOSITION MONITOR
METALLIC IONS	Ca^+, Mg^+, Fe^+	MLTI	DYNAMICS TRACERS

The Ionosphere

- During the day solar radiation ionizes a fraction of the neutral atmosphere.

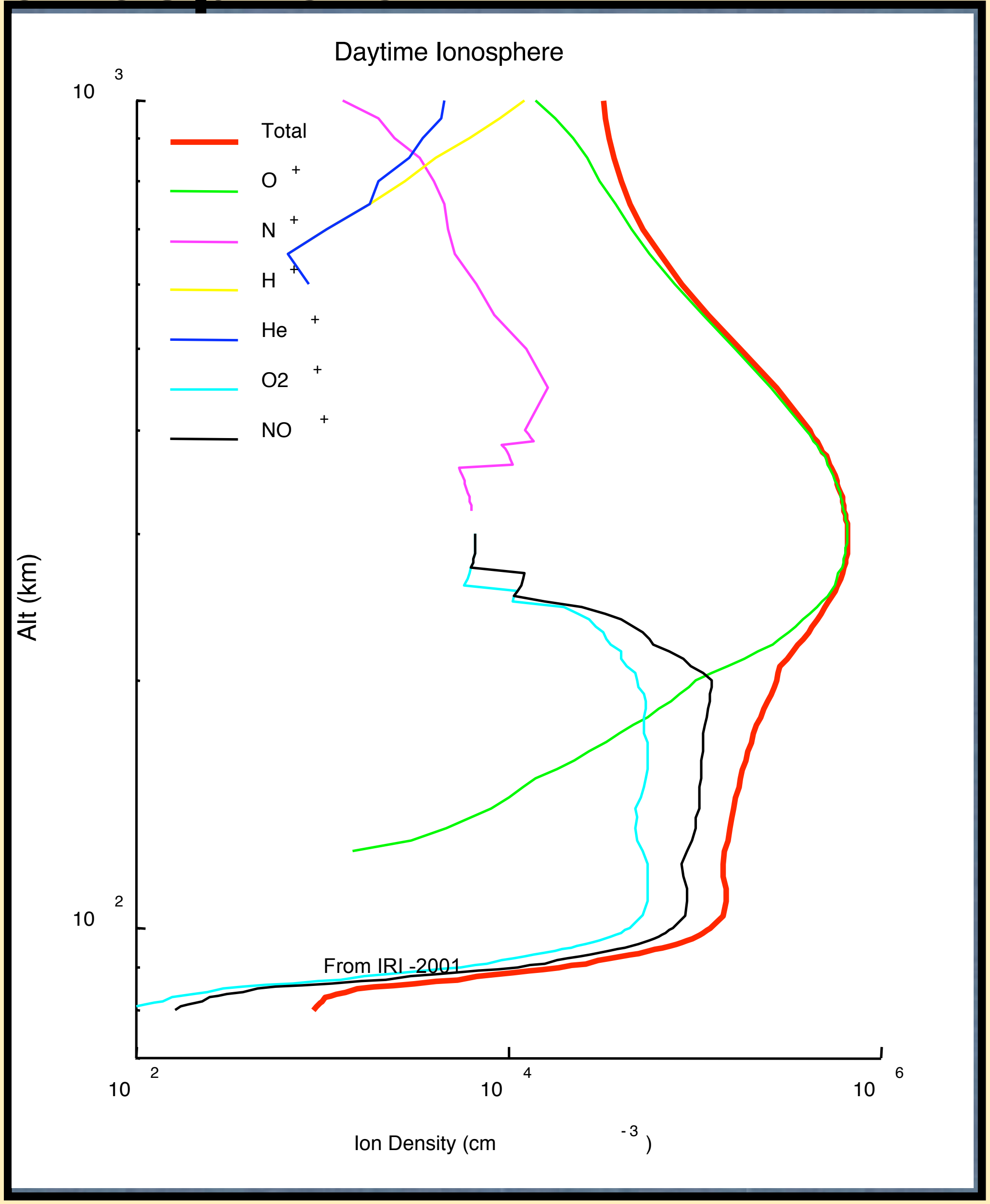

The Ionosphere

- During the day solar radiation ionizes a fraction of the neutral atmosphere.
- At night, ionization is lost mainly through recombination

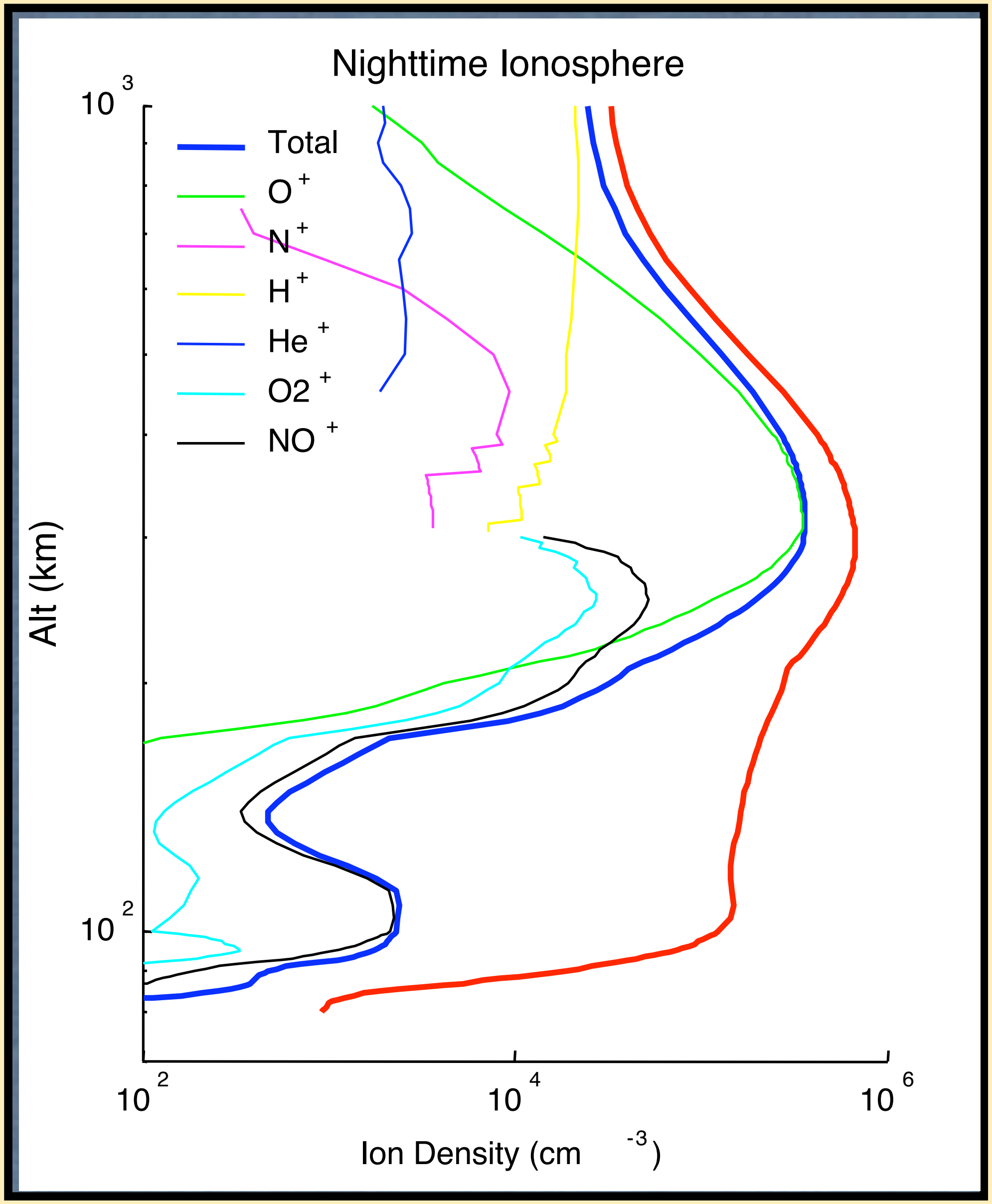

From IRI -2001

Thermosphere vs. Ionosphere

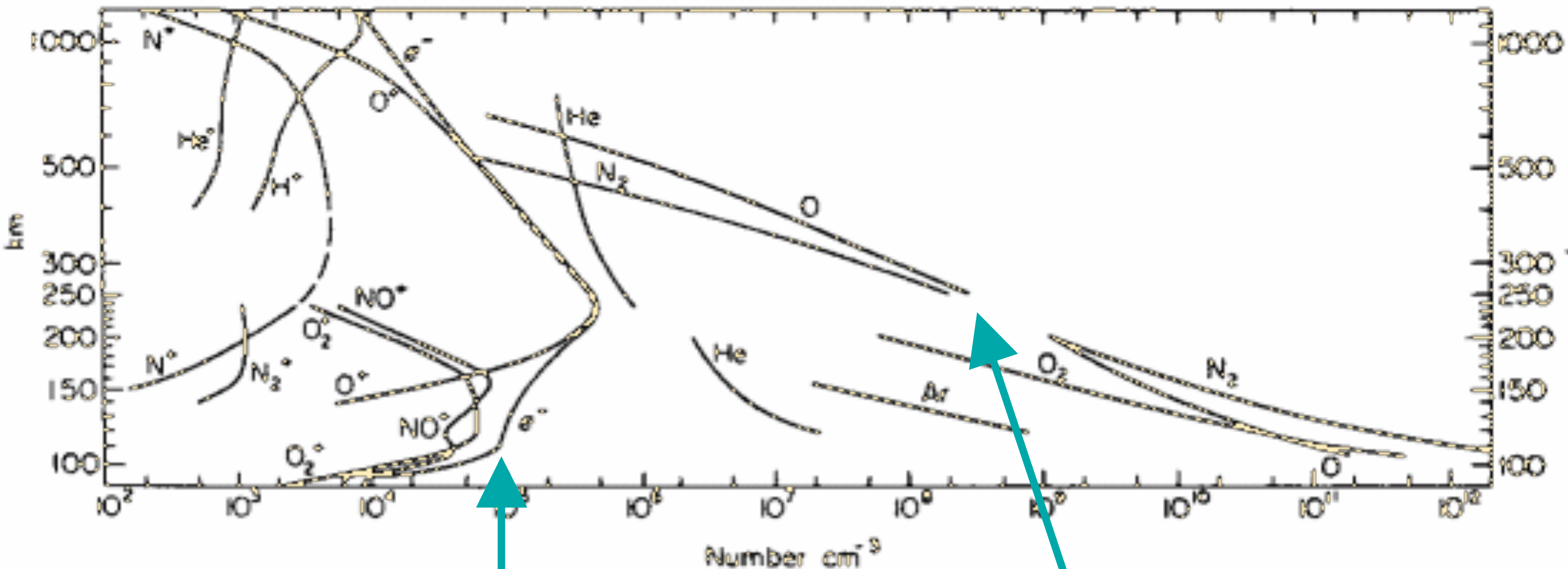

Fig. 1.2. International Quiet Solar Year (IQSY) daytime atmospheric composition, based on

Ionospheric density << Thermospheric density by ~ 1E6

Layers Upon Layers

- Sporadic E
  - Dense: n ~ 10^5
  - Narrow: ~ 5 km in alt
  - Static
  - Metallic
- Intermediate Layers
  - Tenuous: n ~ 10^3-10^4
  - Broad: 10-20 km
  - Descending
  - Molecular (?).

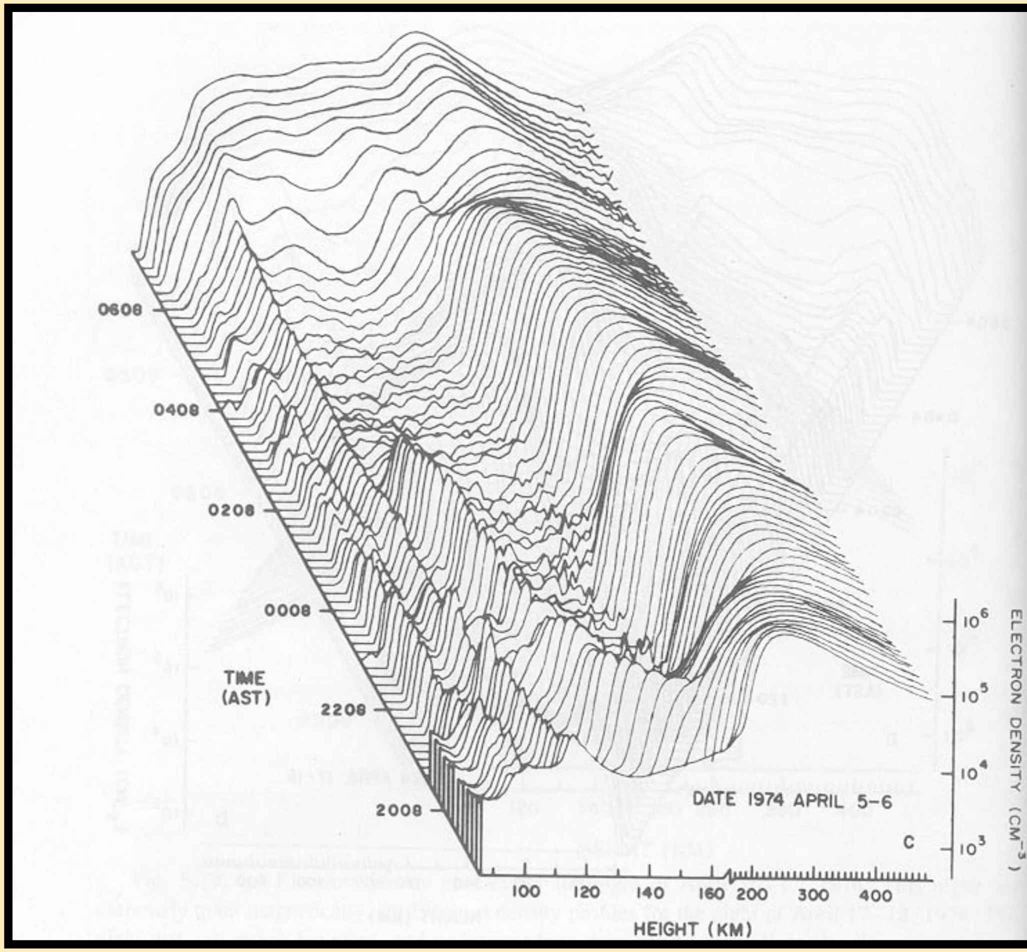

From *Kelley* (1989)

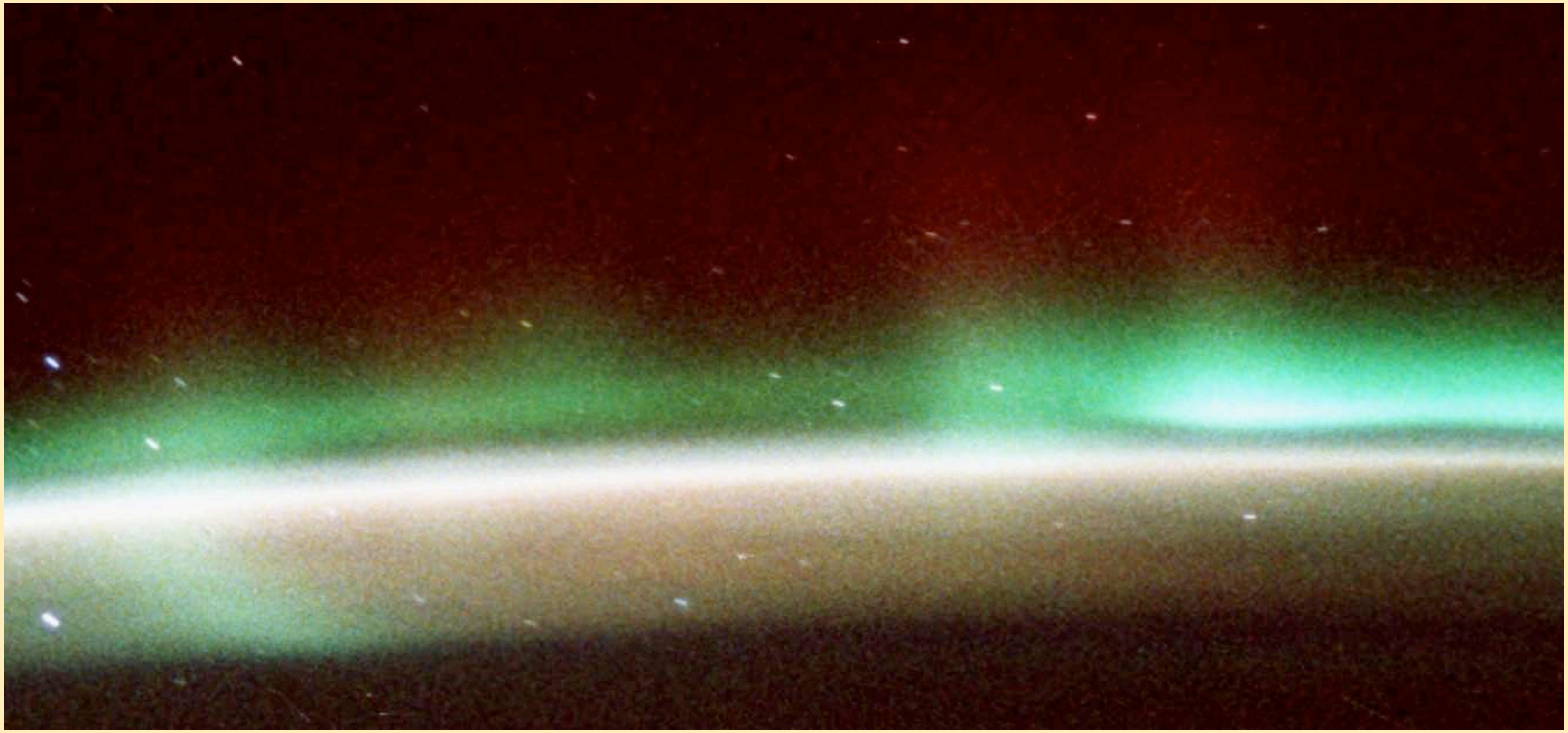

An example of airglow and aurora

The night sky has an overall background luminosity. We are aware of the localized sources of light in a moonless night sky (the stars and planets, the zodiacal light, and gegenschein), but in addition to the astronomical sources there is an overall uniform luminosity originating from the Earth's own atmosphere.

We are not normally aware of this airglow because it is so uniform.

It is the combination of astronomical and airglow sources that allows us to see the silhouette of an object held against the "dark" sky on a clear moonless night.

For a clear moonless night, the nightglow can be seen against the background of stars

Sometime, the nightglow might be so bright that we have what is called a “bright night” and the airglow is actually visible.

Brief Historical Outline

1868	Anders Angstrom discovers green line is present in the night sky even when no aurorae are present
1920's	Robert John Strutt (4th Baron Rayleigh) begins investigations [Note: he is referred to as the "airglow Rayleigh"; his father John William Strutt, 3rd Baron Rayleigh, is the "scattering Rayleigh"]
1923	John McLennon & G.M. Shrum identify green line to be due to atomic oxygen
1929	Vesto Melvin Slipher discovers sodium layer (a contribution to airglow)
1931	Sydney Chapman suggests airglow is result of chemical recombination
1939	Chapman suggests reaction cycle to sustain sodium nightglow
1950	term "airglow" coined after other atmospheric emissions are identified
1956	SAR arc discovered by Barbier over France

The Rayleigh is a unit of surface brightness

1 R $=10^{10}$ photons/(m^2column)/sec/ster or
$1.58\times10^{-11}/\lambda$ W (cm^2column)/sec/ster
where λ is the wavelength in nm.

The surface brightness for an extended source is independent of the distance of the observer and is represented by the column (of unit cross section) integration of the omni-directional volume emission rate within the extended airglow layer.

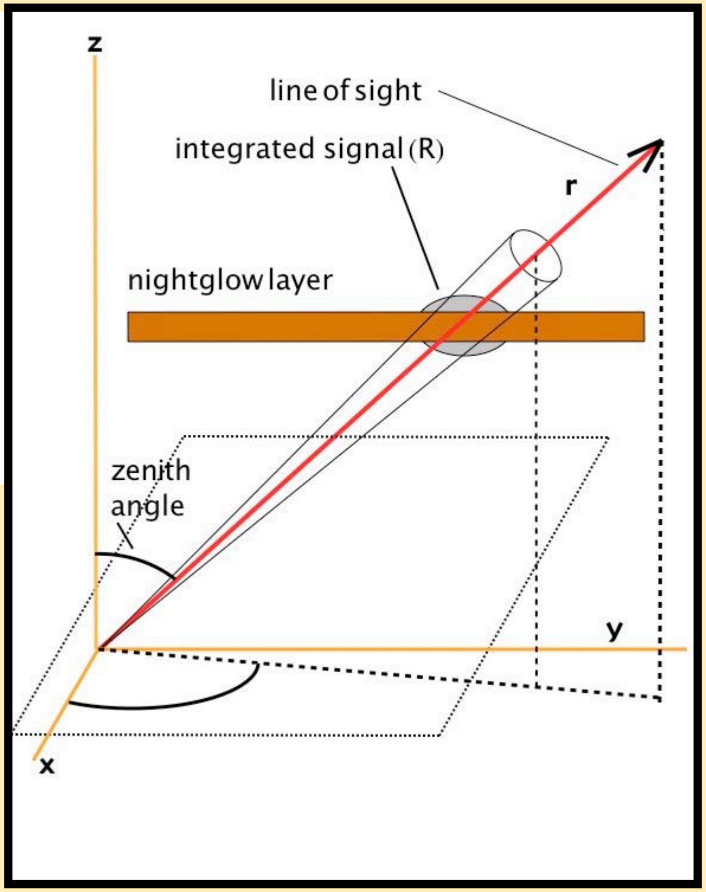

Typical airglow brightnesses 10-100 R
auroral 1-100 kR

Airglow production processes are divided into three types:

- *Dayglow* (when entire atmosphere is illuminated by the Sun) is the brightest airglow due to the importance of RESONANT and FLUORESCENT processes (described next) but it is overwhelmed by direct and scattered sunlight

- *Twilightglow* (when only the upper atmosphere is illuminated) is the most readily-observable airglow from the ground since the observer is in darkness (and Rayleigh scattering of sunlight by the dense lower atmosphere is absent) while the airglow region of upper atmosphere is still illuminated

- *Nightglow* (when entire atmosphere is in darkness) is not as bright as dayglow and CHEMILUMINESCENCE (see below) is the dominant process;

however, the nightglow contributes more light than starlight
to the total luminosity of the night sky

CHEMILUMINESCENCE:

emissions result from chemical reactions mainly between oxygen and nitrogen atoms and molecules and OH molecules at a height between 100 and 300 km.

Solar radiation energy breaks molecules apart during the day, and it is their recombination, which is accompanied by the emission of light, that generates the nightglow.

$H + O_3 \Rightarrow OH^* + O_2$

$OH^* \Rightarrow OH^{**} \Rightarrow OH^{***}$

OH rotational-vibronic emissions very prevalent within the visible spectral region.

Table 2.2 Emissions of some excited species in the middle atmosphere

Lower state	Excited state	Radiative lifetime (s)	λ (angstrom)	Name
$O(^3P)$	$O(^1D)$	110	6300	Red line
$O(^1D)$	$O(^1S)$	0.74	5577	Green line
$O_2(X^3\Sigma_g^-)$	$O_2(a^1\Delta_g)$	2.7(3)	12700+	Infrared atmospheri bands
$O_2(X^3\Sigma_g^-)$	$O_2(b^1\Sigma_g^+)$	12	7619+	Atmospheric bands
$O_2(X^3\Sigma_g^-)$	$O_2(A^3\Sigma_u^+)$	1	2600-3800	Herzberg bands
$OH(X^2\Pi)_{v=0,1,..}$	$OH(X^2\Pi)_{v=9,8,..}$	6(-2)	<28007	Meinel bands
$N(^4S)$	$N(^2D)$	9.36(4)	5200	
$N(^4S)$	$N(^2P)$	12	3466	
$N_2(X^1\Sigma_g^+)$	$N_2(A^3\Sigma_u^+)$	2	2000-4000	Vegard-Kaplan bands
$NO(X^2\Pi)$	$NO(A^2\Sigma^+)$	2(-7)	2000-3000	γ bands

Imaging spectrograph

- Spectral content represented by molecular rotational, vibrational, and electronic transitions
- Dispersive element of grating
- CCD detector now generally applied
- Modern day technology extremely powerful compared with spectral instruments pre-CEDAR times

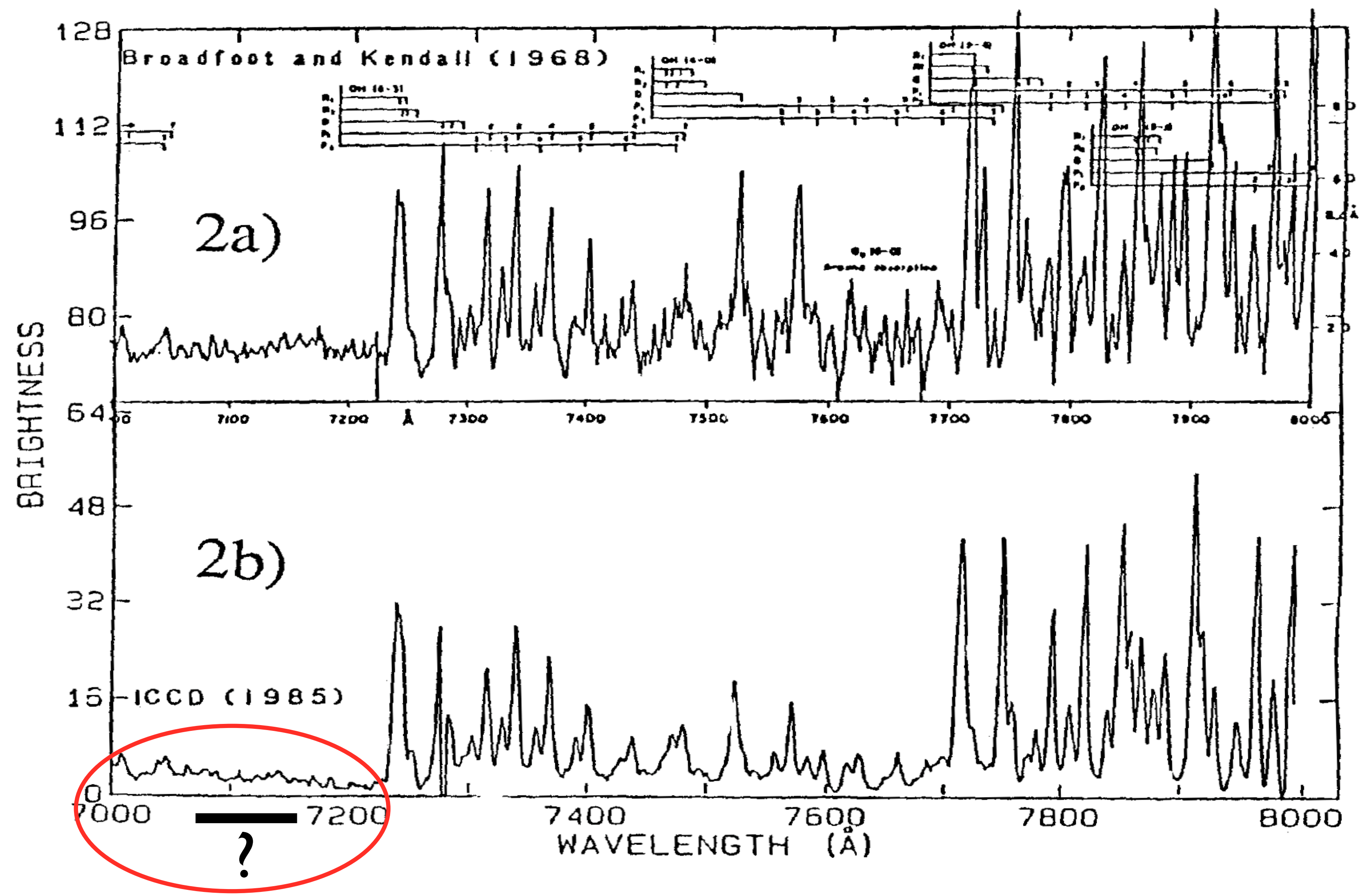

'ig. 2*a*. Airglow spectra obtained by Broadfoot at Kitt Peak with a 1m spectrophotometer [*Broadfoot and Kendall*, 968], and (b), airglow spectra obtained by L. B. Broadfoot at Kitt Peak with a 0.5 m charge coupled device imaging pectrograph. Only a few minutes integration was necessary [from *Sharp*, 1986].

A nightglow spectrum obtained by a Fastie-Ebert spectrometer - 1960s technology - compared with the 1985 spectrum obtained by a CEDAR-funded specgtrograph - note mystery region near 710 nm

An example of today's technology obtained with the Keck telescope high resolution spectrograph

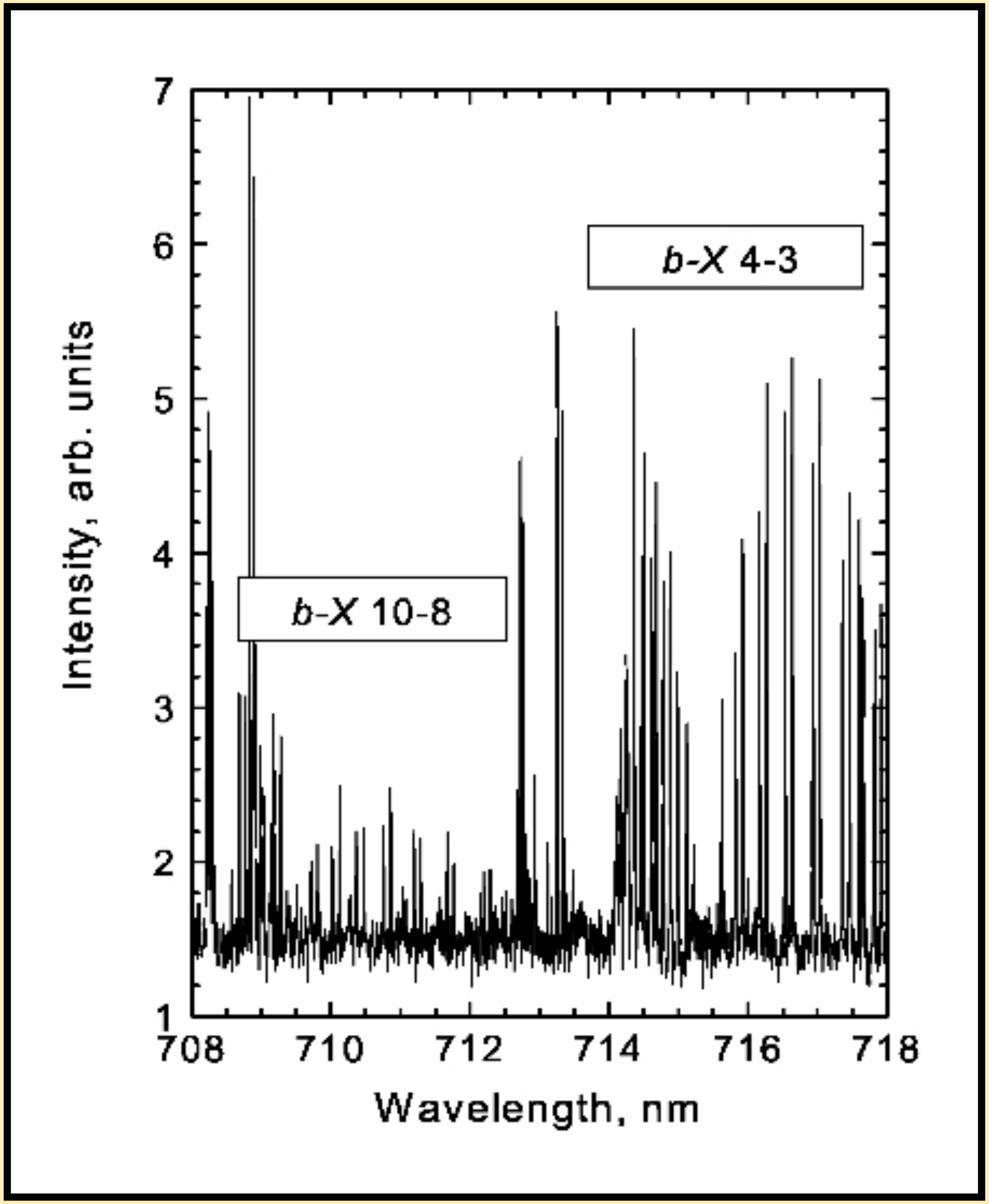

Modern spectrograph technology can observe very weak spectral features in the nightglow.

The Keck telescope gets excellent nightglow spectra every night!

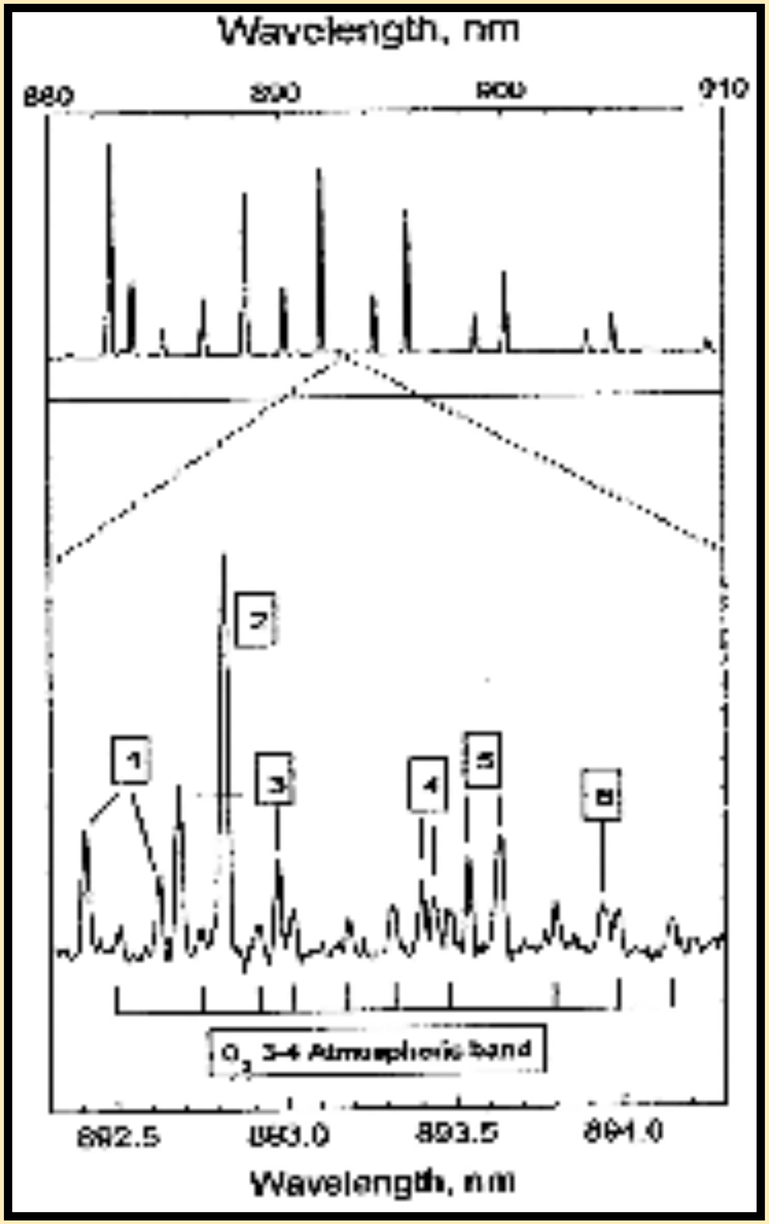

Visible spectrum of the aurora:
dominant features are oxygen green and red lines

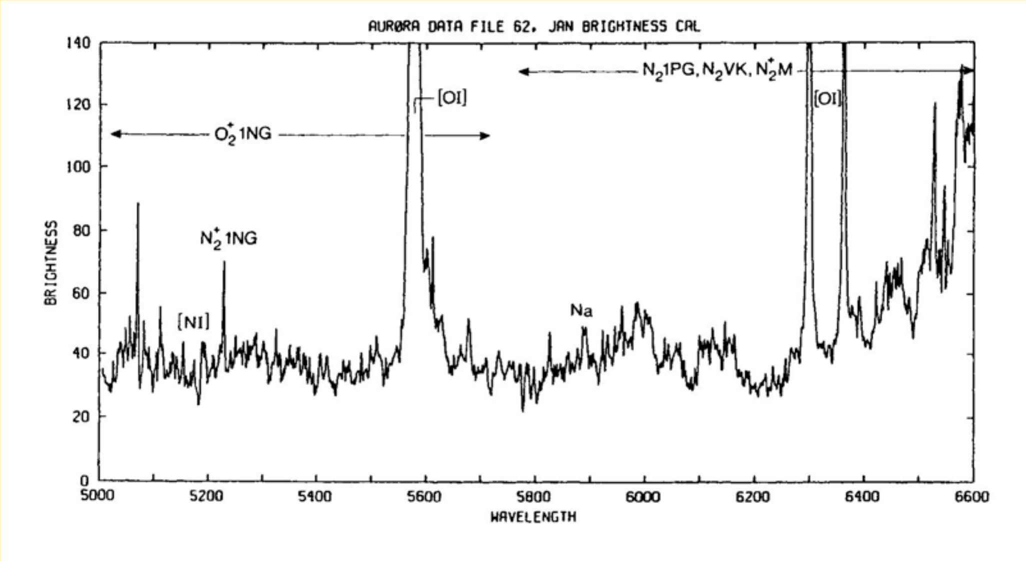

O(1S) $\rightarrow$ O(1D) ‚green line'
O(1D) $\rightarrow$ O(3P) ‚red lines'

excitation mechanism:

electron impact	O + e	$\rightarrow$ O* + e
energy transfer	$N_2(^3\Sigma_u)$ + O(3P)	$\rightarrow$ O(1S) + $N_2(^1\Sigma_g)$
radiative recombination	O_2^+ + e	$\rightarrow$ 2 O(3P,1D,1S)
ion reactions	$N^+ + O_2$	$\rightarrow$ NO^+ + O(1S)
	$O2^+$ + N	$\rightarrow$ NO^+ + O(1S)